TASTE

- FUNCTIONS → nutrition – survival

  → Information on toxicity and sugar content

- basic tastes

  sweetness: sugar (energy)
  bitterness: plant alcaloids, toxins (dangerous, unpleasant, sharp, or disagreeable)
  saltiness: sodium ions (osmoregulation)
  sourness: acidity (unripe fruits, spoiled food)
  umami: proteins (meaty)

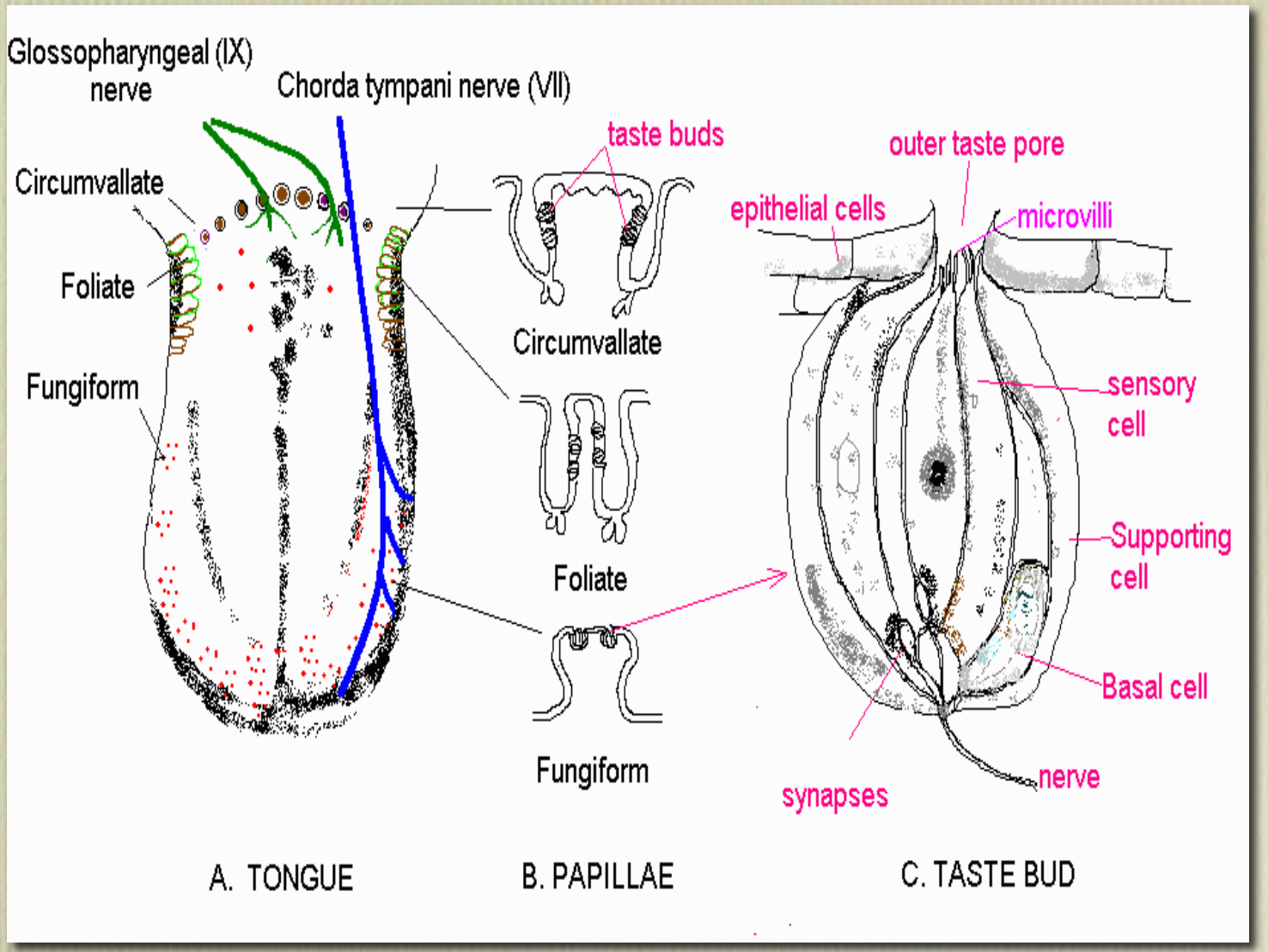
Glossopharyngeal (IX) nerve
Chorda tympani nerve (VII)
Circumvallate
Foliate
Fungiform
taste buds
Circumvallate
Foliate
Fungiform
outer taste pore
epithelial cells
microvilli
sensory cell
Supporting cell
Basal cell
synapses
nerve
A. TONGUE
B. PAPILLAE
C. TASTE BUD

Thermal Gating of TRP Ion Channels: Food for Thought?

Emily R. Liman*

(Published 14 March 2006)

Science's stke

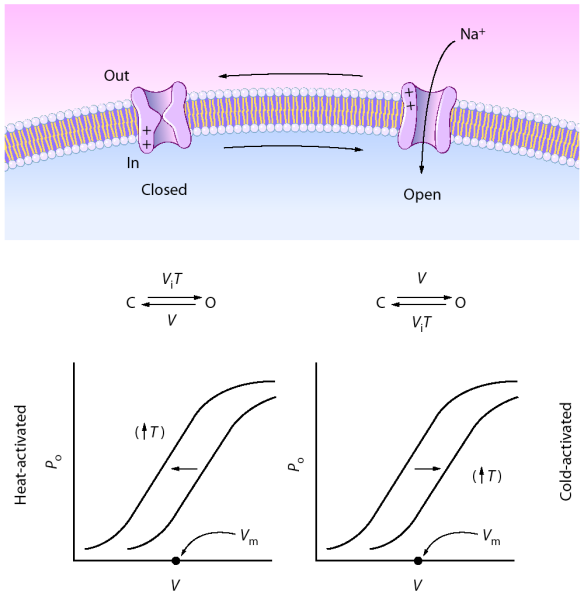

Fig. 1. Model for thermal gating of TRP channels. In this simple model, the channel can occupy one of two states—closed and open—and transitions between the two states are sensitive to voltage (depolarization promotes entry into the open state). Thermosensitivity of the channel results from an asymmetry in the temperature dependence of opening and closing transitions. For the heat-activated channels, the opening transition is more temperature sensitive, whereas for cold-activated channels, the closing transition is more temperature sensitive. This model predicts that the probability that channels are open (Po) as a function of voltage (V) shifts to the left upon warming for TRPV1 and to the right for TRPM8, a prediction that is validated by the data [based on (*10*, *11*)]. See (*12*) for an alternate allosteric model for thermo-gating of TRPM8.

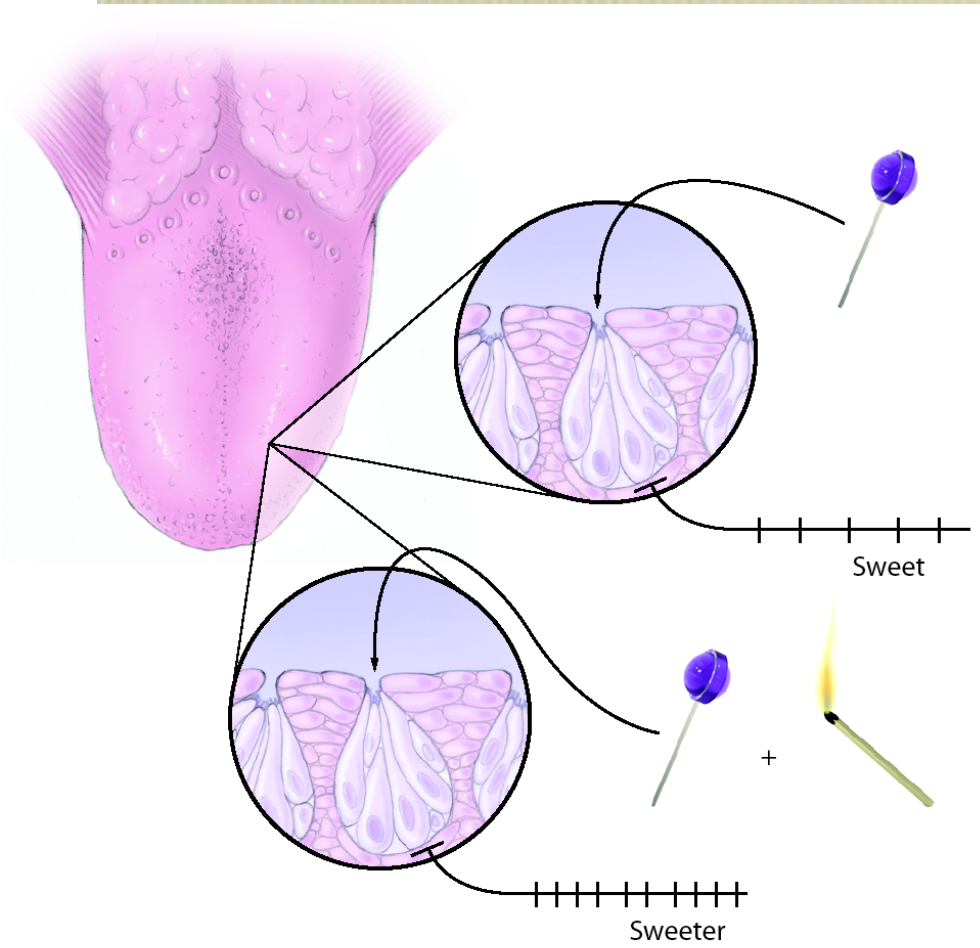

Fig. 2. Signaling of sweet taste is enhanced at warm temperatures. The frequency of action potentials in gustatory nerves in response to sweet chemicals is increased at warmer temperatures. TRPM5 channels are essential for sweet taste, and it is hypothesized that the increased activity of TRPM5 channels at warm temperatures underlies thermal sensitivity of sweet taste (*5*).

taste buds

- Not only in tongue but also in pharynx, larynx and esophagous
- Each bud includes
  - 50-150 taste cells
  - Basal cells (precursors)
  - Supporting cells
  - Nerve fibers
- 2000/5000 buds/person

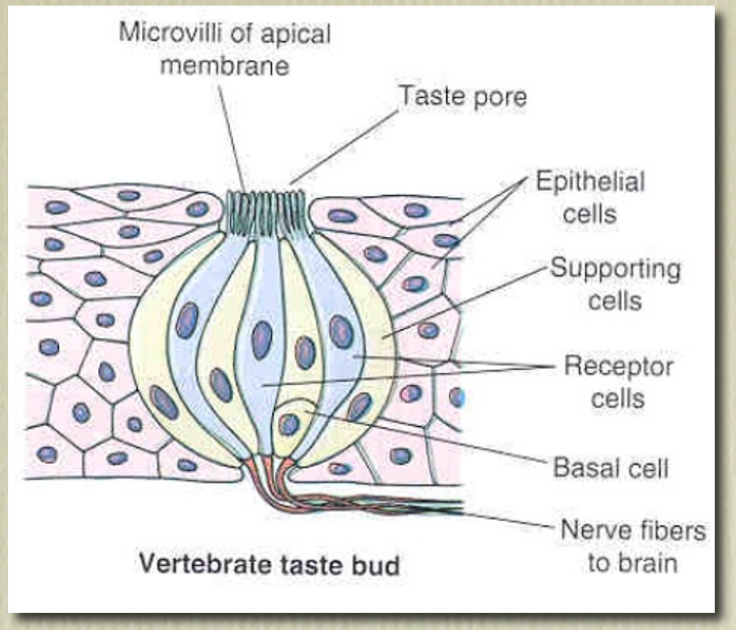

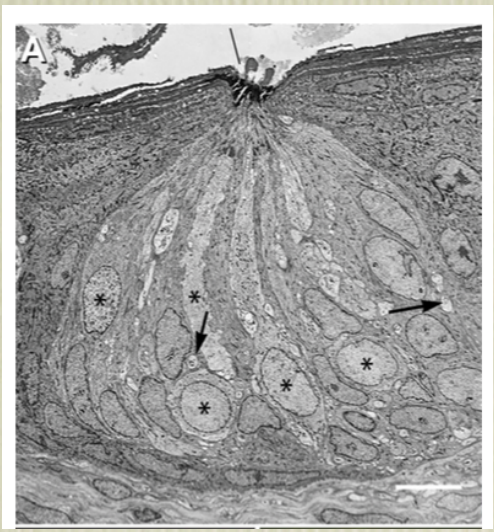

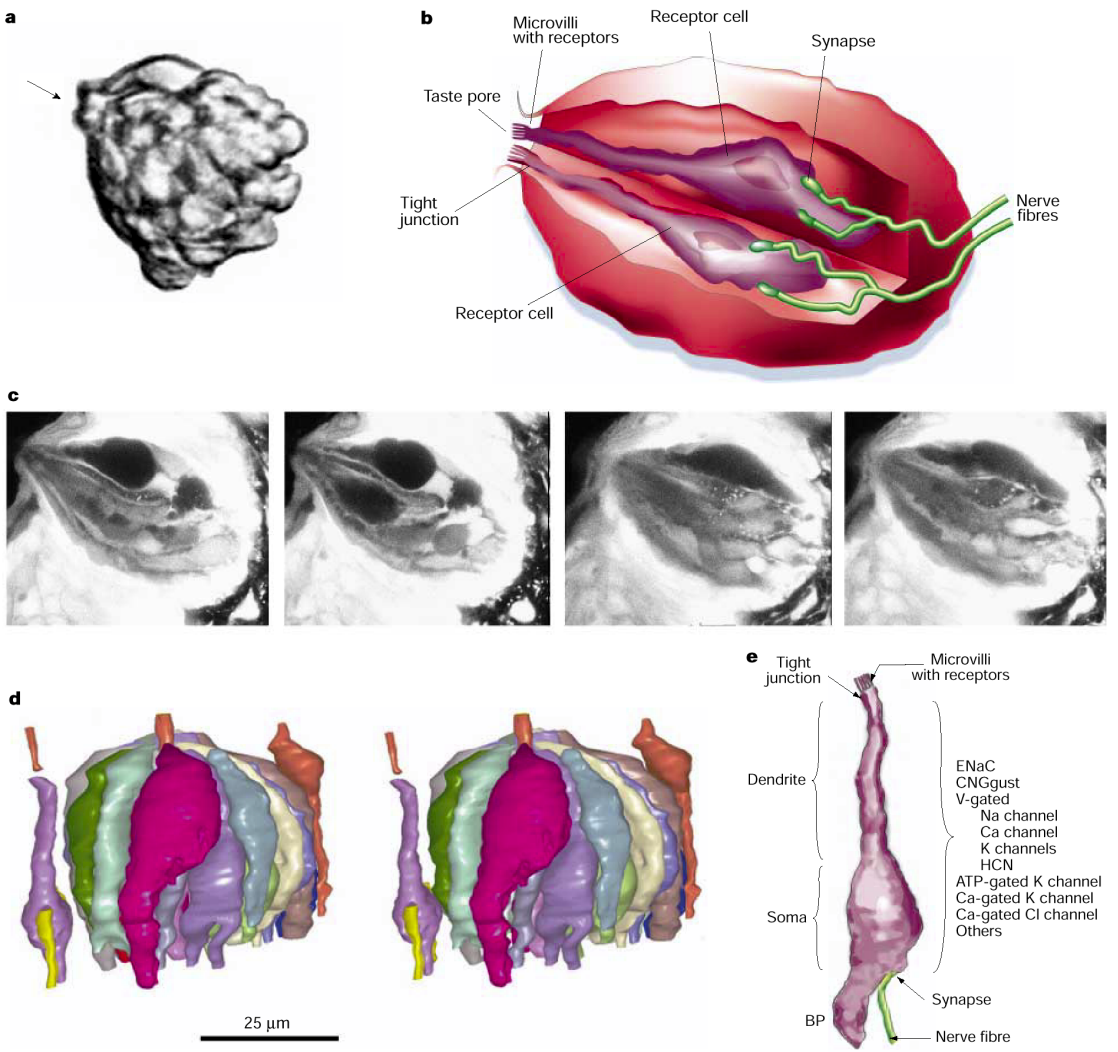

Figure 1 Morphology of taste buds (rat). **a**, Viable bud isolated from the vallate papilla. Taste pore at the upper left (arrow). Length of bud is 30 µm. **b**, Cut-open view of a bud (cartoon). Highlighted are two receptor cells with apical microvilli and basolateral synapses. **c**, Images of a viable bud from the vallate papilla, taken with a 2-photon microscope. The four optical planes depict multiple bipolar cells in different states of loading with a fluorescent dye, and nerve fibres. **d**, Three-dimensional reconstruction, from microscopic serial sections, of a bud from the foliate papilla, the taste pore facing upwards. On the left, a solitary bipolar cell with innervating nerve fibre is also visible. Scale bar, 25 µm. (Image courtesy of V. I. Popov, Institute of Cell Biophysics, RAS, Pushchino, Russia.). **e**, Bipolar receptor cell with sensory nerve fibre attached. Some morphological details and the location of the main types of identified ion channels on the lateral membrane are indicated. BP, basal cell process.

Review series

The cell biology of **taste**

Nirupa Chaudhari and Stephen D. Roper

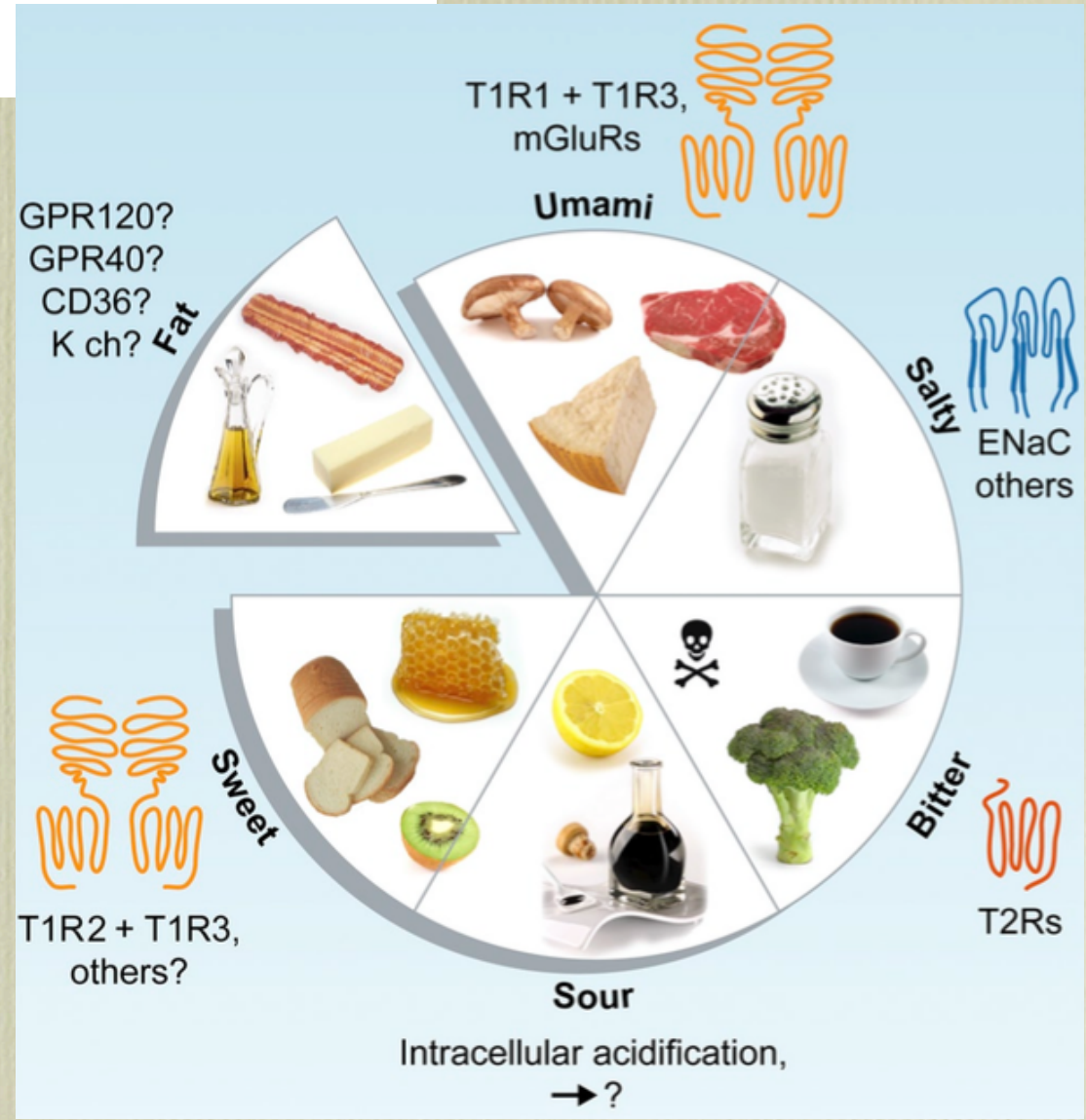

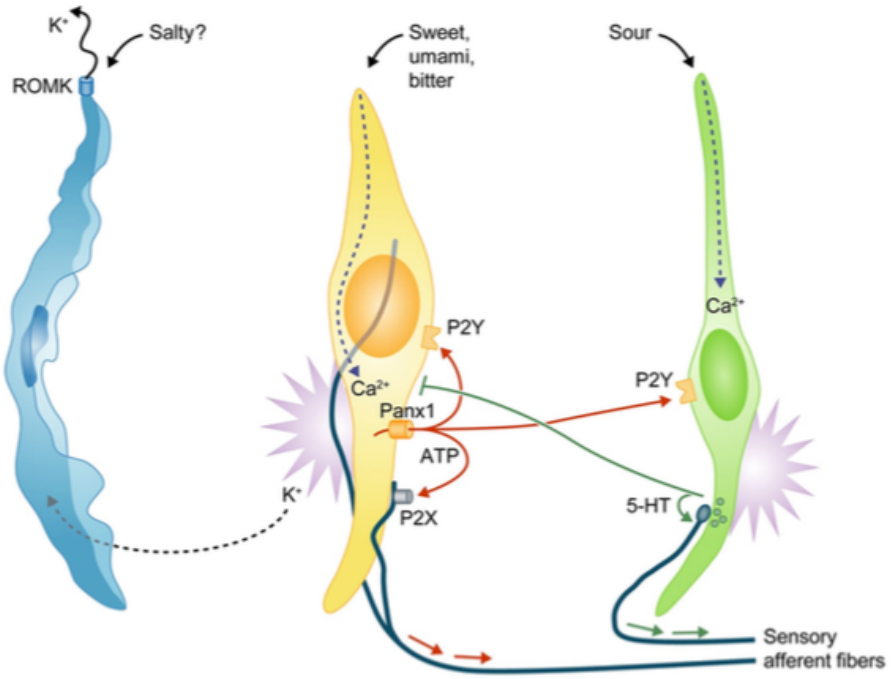

Type I glial-like cell	
Neurotransmitter clearance	
GLAST	Glutamate reuptake
NTPDase2	Ecto-ATPase
NET	Norepinephrine uptake
Ion redistribution and transport	
ROMK	K^+ homeostasis
Other	
OXTR	Oxytocin signaling?

Type II receptor cell	
Taste transduction	
T1Rs, T2Rs	Taste GPCRs
mGluRs	Taste GPCRs
Gα-gus, Gγ13	G protein subunits
PLCβ2	Synthesis of IP3
TRPM5	Depolarizing cation current
Excitation and transmitter release	
$Na_v1.7$, $Na_v1.3$	Action potential generation
Panx1	ATP release channel

Type III presynaptic cell	
Surface glycoproteins, ion channels	
NCAM	Neuronal adhesion
PKD channels	Sour taste?
Neurotransmitter synthesis	
AADC	Biogenic amine synthesis
GAD67	GABA synthesis
5-HT	Neurotransmitter
Chromogranin	Vesicle packaging
Excitation, transmitter release	
$Na_v1.2$	Action potential generation
$Ca_v2.1$, $Ca_v1.2$	Voltage-gated Ca^{2+} current
SNAP25	SNARE protein, exocytosis

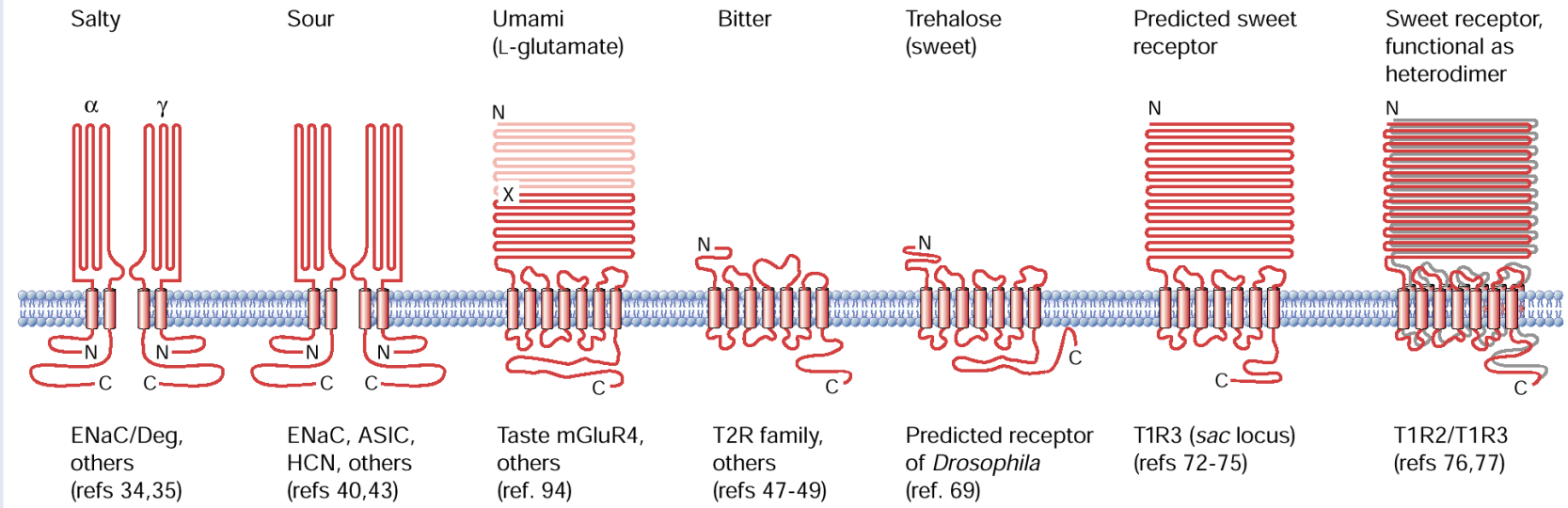

Figure 2 Taste receptors of known primary structure, discovered 1998–2001.

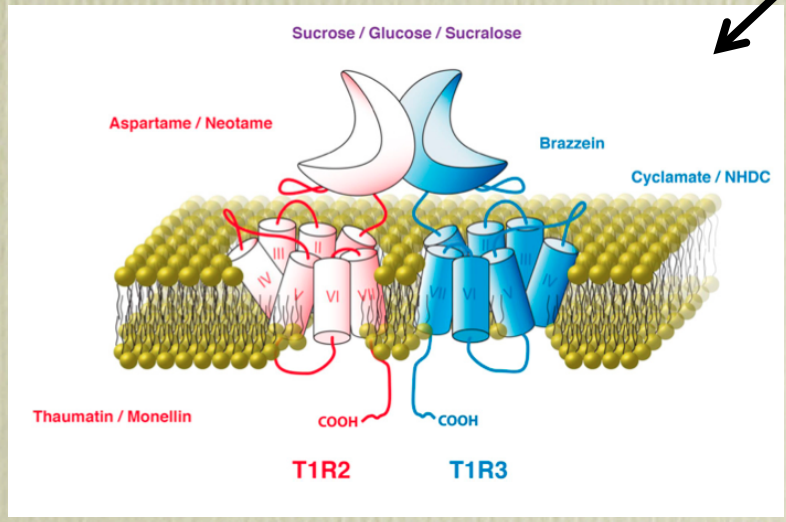

TRCs subtypes express different molecular patterns

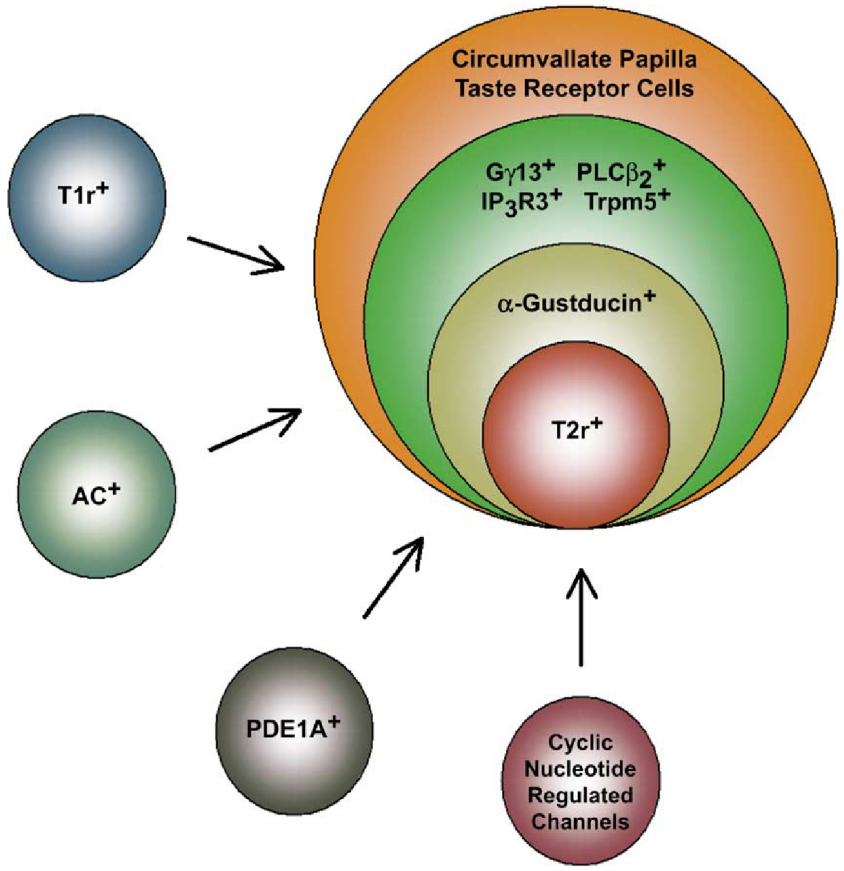

Fig. 4. Diagram of TRC subsets according to expression of signaling molecules. Gene expression profiling, in situ hybridization and immunohistological studies indicate the following pattern of co-expression for the molecules α-gustducin, Gγ13, PLCβ2, IP_3R3 and Trpm5 in circumvallate taste buds. Note the absolute co-expression of Gγ13, PLCβ2, IP_3R3 and Trpm5. α-Gustducin is expressed in a subset of these TRCs. T2r receptors are expressed in a subset of α-gustducin$^+$ TRCs. Additional TRC subsets will be defined as more comprehensive studies on the co-expression of the above mentioned molecules and other signaling elements such as sweet/*umami* taste receptors (T1r), G proteins subunits and effectors (PDE1A, adenylyl cyclase (AC)) are carried out. Modified from [37] with permission from the authors.

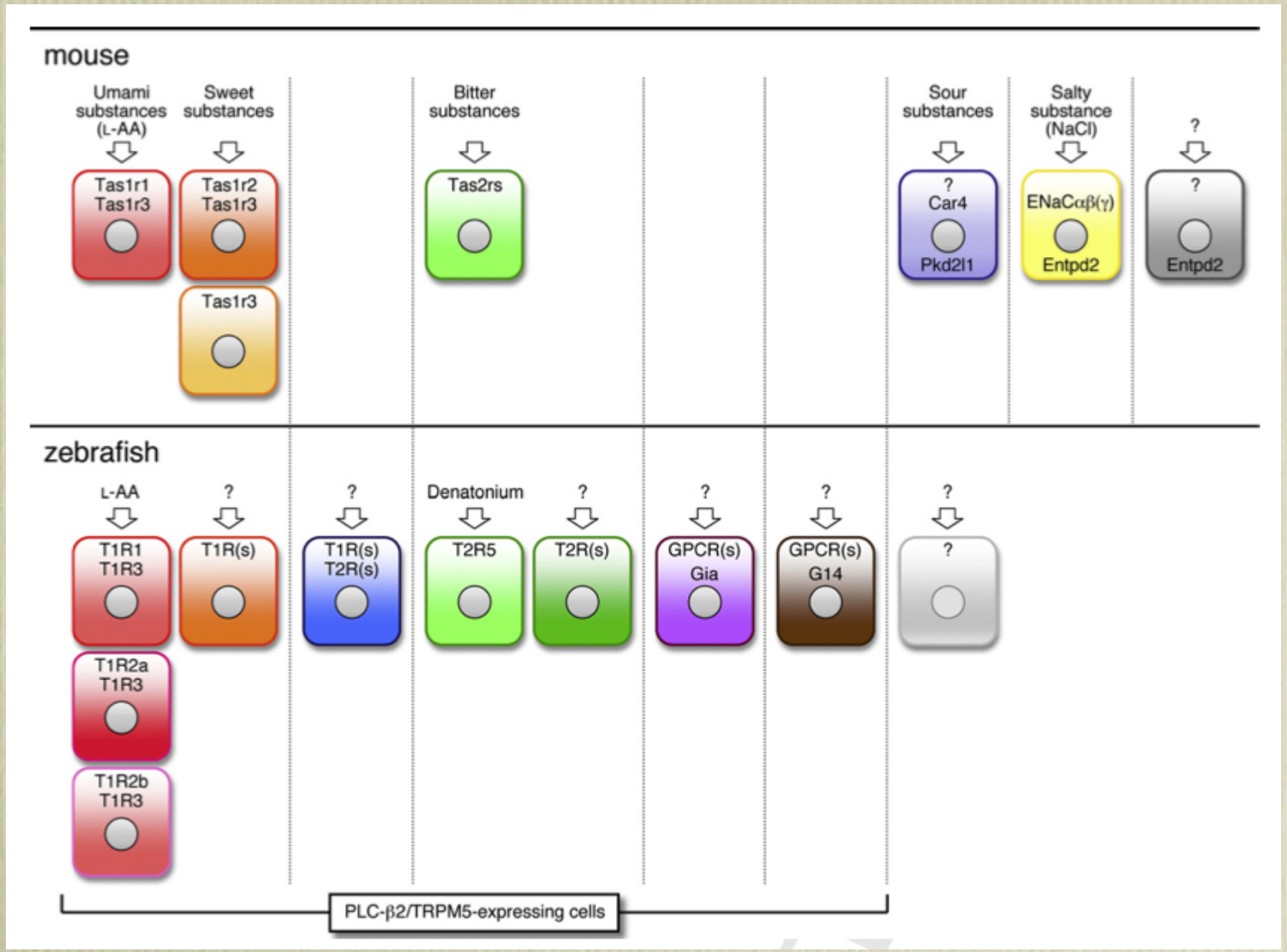
mouse
Umami substances (L-AA)
Sweet substances
Bitter substances
Sour substances
Salty substance (NaCl)
?
Tas1r1 Tas1r3
Tas1r2 Tas1r3
Tas1r3
Tas2rs
? Car4 Pkd2l1
ENaCαβ(γ) Entpd2
? Entpd2
zebrafish
L-AA
?
?
Denatonium
?
?
?
?
T1R1 T1R3
T1R(s)
T1R(s) T2R(s)
T2R5
T2R(s)
GPCR(s) Gia
GPCR(s) G14
?
T1R2a T1R3
T1R2b T1R3
PLC-β2/TRPM5-expressing cells

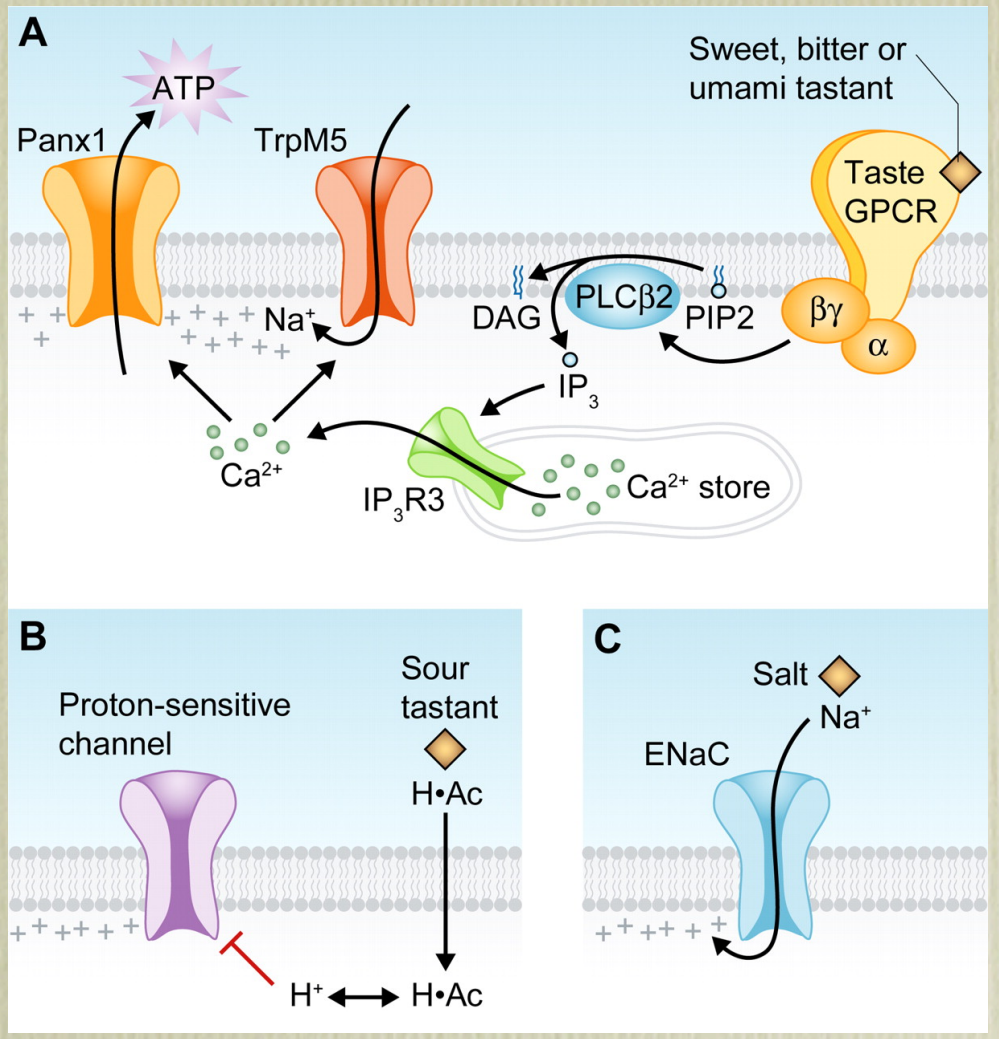

Chaudhari N , Roper S D J Cell Biol 2010;190:285-296

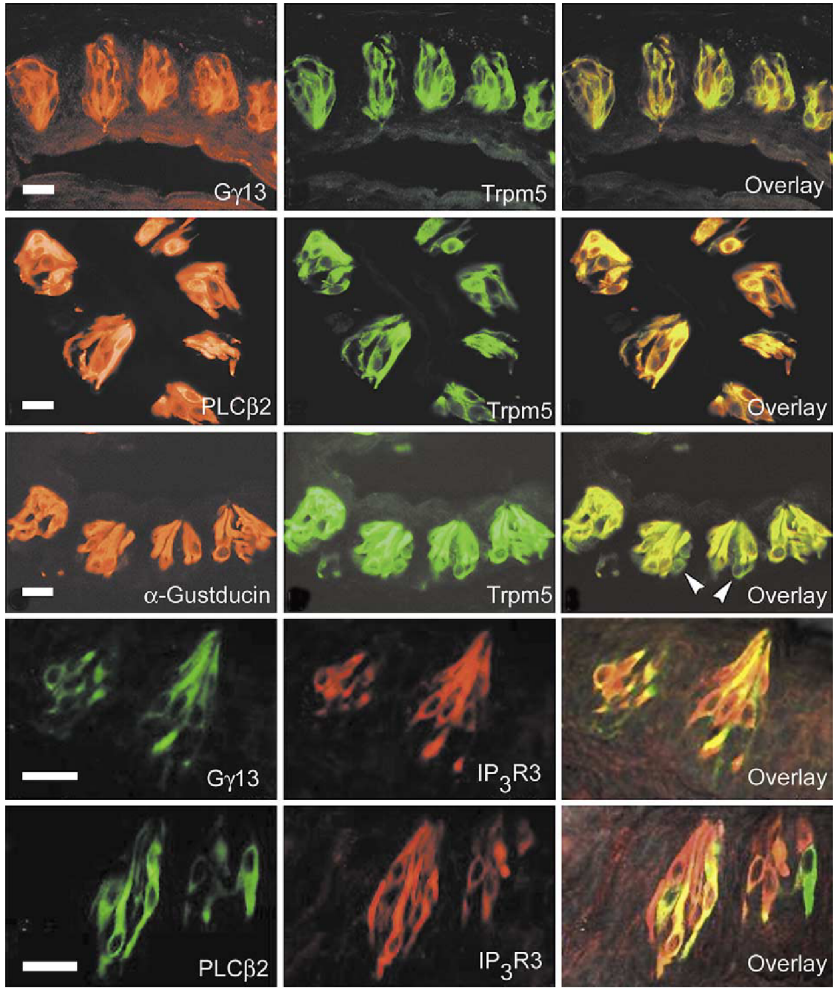

Fig. 3. Co-expression of Trpm5 and IP_3R3 with TRC signaling molecules. Immunohistological staining of CV papillae tissue showing the co-expression of Trpm5 and IP_3R3 with Gγ13, PLCβ2 and α-gustducin. Additionally we have directly confirmed the coexpression of Trpm5 and IP_3R3 (Todd Clapp, RFM and SCK, data not shown). Scale bar = 20 μm. Reproduced from [37,69] with permission from the authors.

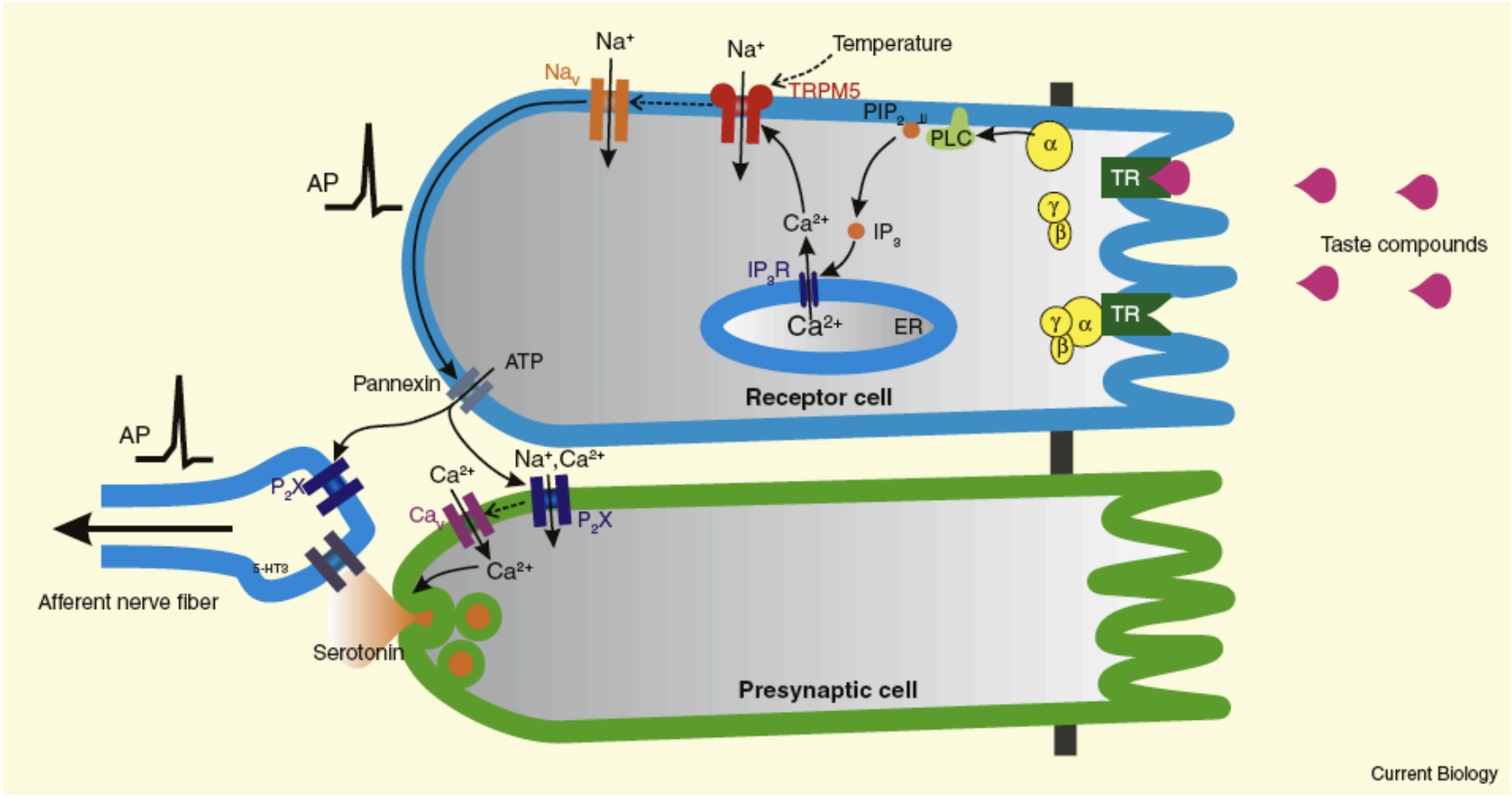

Figure 2. Model for the role of TRPM5 in the perception of sweet, bitter or umami taste.

In taste receptor cells of the tongue, taste compounds bind to G-protein-coupled taste receptor proteins (TRs), evoking bitter, sweet or umami taste sensation. These TRs include dimeric T1R2 + T1R3 for sweet taste and more than 36 T2Rs for bitter taste (for a review, see [36]). TRs activate phospholipase C (PLC) via the G protein α subunit α-gustducin, leading to the production of inositol 1,4,5-trisphosphate (IP_3) and release of Ca^{2+} from intracellular stores via the IP_3 receptor (IP_3R). The rise in intracellular Ca^{2+} opens TRPM5, leading to membrane depolarization, activation of voltage-gated Na^+ (Na_V) channels and generation of action potentials (AP). The depolarization results in the release of ATP, probably via pannexin-type hemichannels. The released ATP activates ionotropic purinergic (P_2X) receptors on neighboring presynaptic cells, leading to depolarization, activation of voltage-gated Ca^{2+} (Ca_V) channels and Ca^{2+}-dependent exocytosis of serotonin-containing vesicles. Afferent sensory fibers are depolarized by the serotonin release from the presynaptic cells (via ionotropic 5-HT3 receptors) and possibly by the ATP released from the taste receptor cells (via P_2X receptors).

TRPM5 is also expressed in olfactory neurons…feromones

nature Vol 438|15 December 2005|doi:10.1038/nature04248

LETTERS

Heat activation of TRPM5 underlies thermal sensitivity of sweet taste

Karel Talavera[1], Keiko Yasumatsu[2], Thomas Voets[1], Guy Droogmans[1], Noriatsu Shigemura[2], Yuzo Ninomiya[2], Robert F. Margolskee[3] & Bernd Nilius[1]

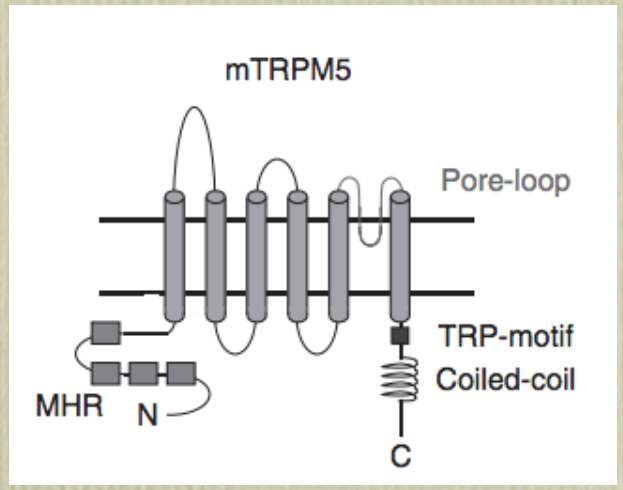

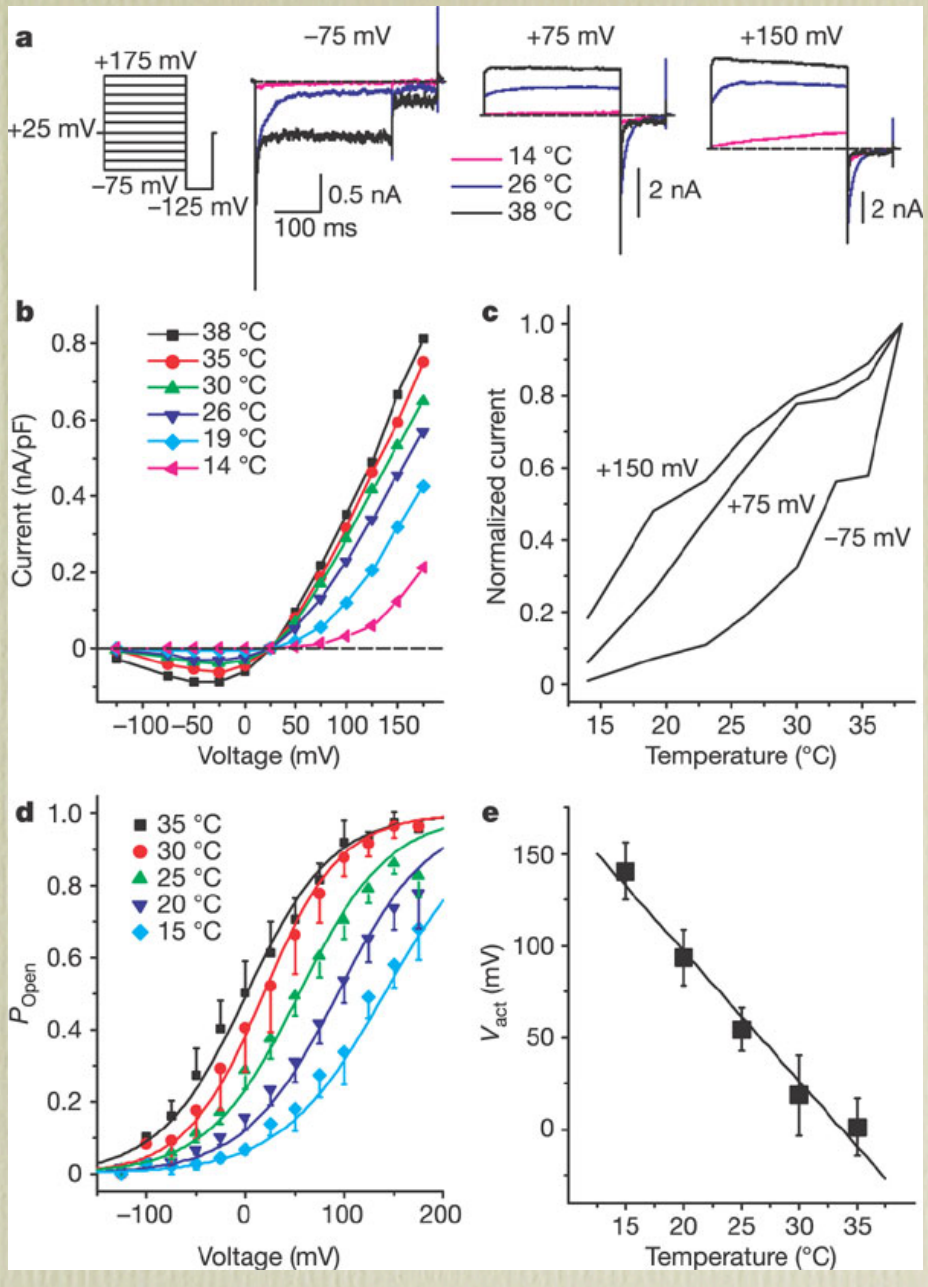

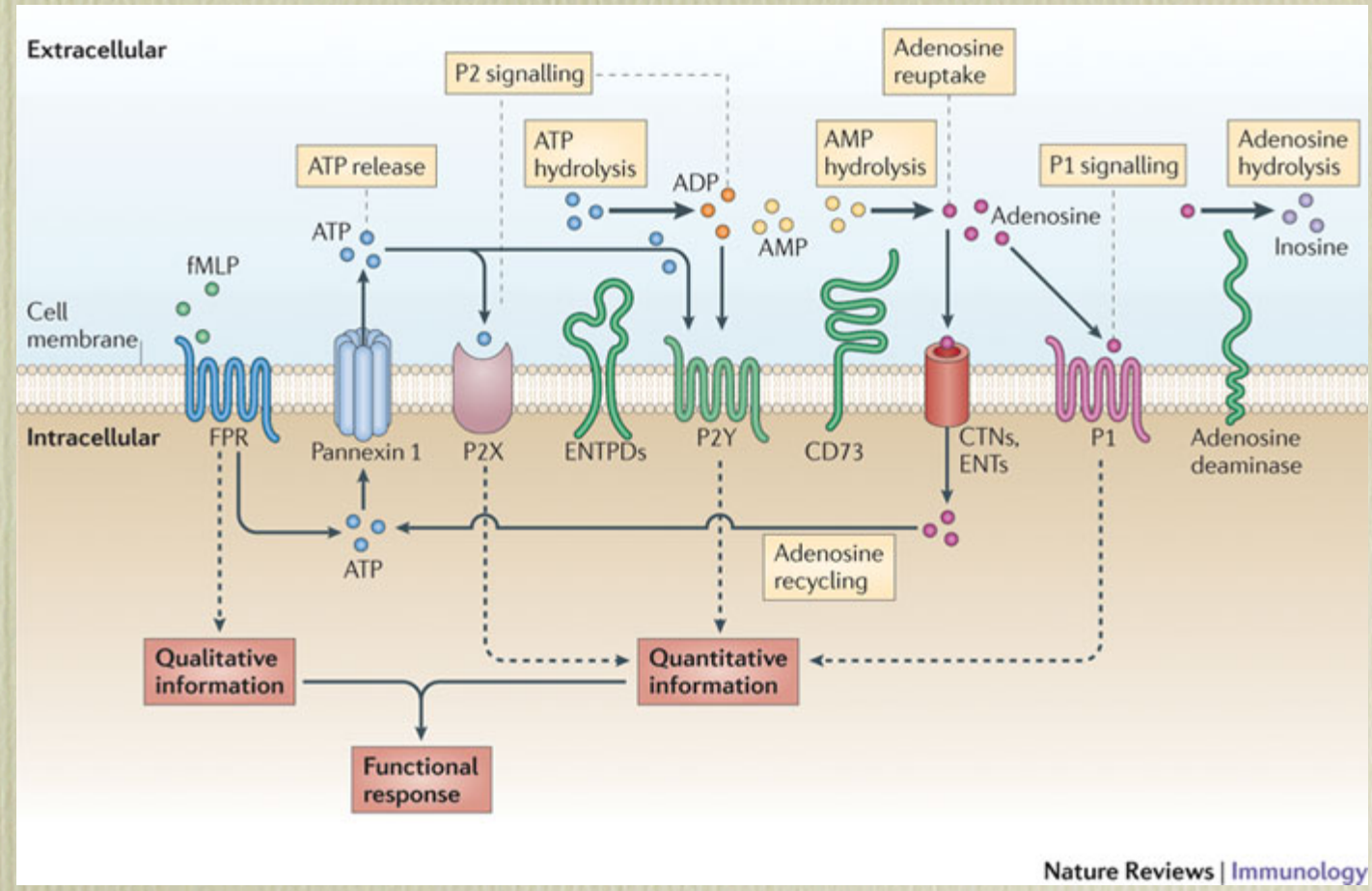
Extracellular
P2 signalling
Adenosine reuptake
ATP release
ATP hydrolysis
AMP hydrolysis
P1 signalling
Adenosine hydrolysis
ADP
ATP
AMP
Adenosine
Inosine
fMLP
Cell membrane
Intracellular
FPR
Pannexin 1
P2X
ENTPDs
P2Y
CD73
CTNs, ENTs
P1
Adenosine deaminase
ATP
Adenosine recycling
Qualitative information
Quantitative information
Functional response
Nature Reviews | Immunology

pannexins

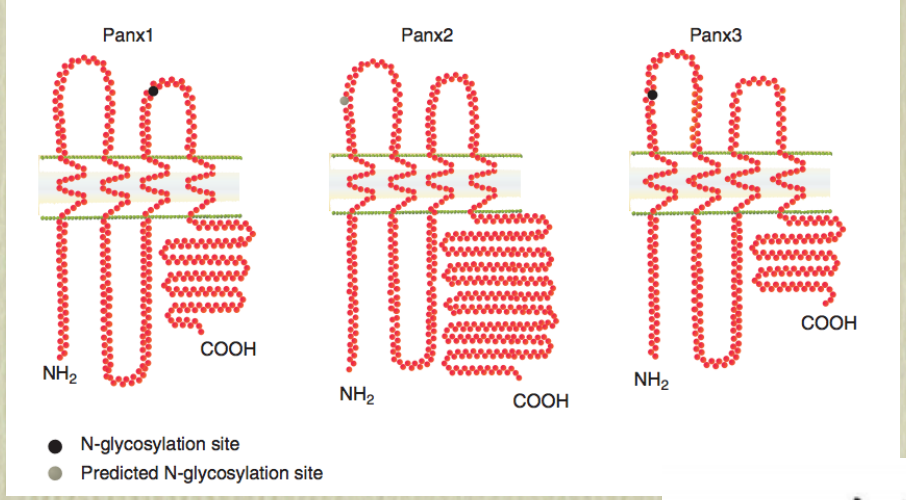
Panx1
Panx2
Panx3
NH2
COOH
NH2
COOH
NH2
COOH
N-glycosylation site
Predicted N-glycosylation site

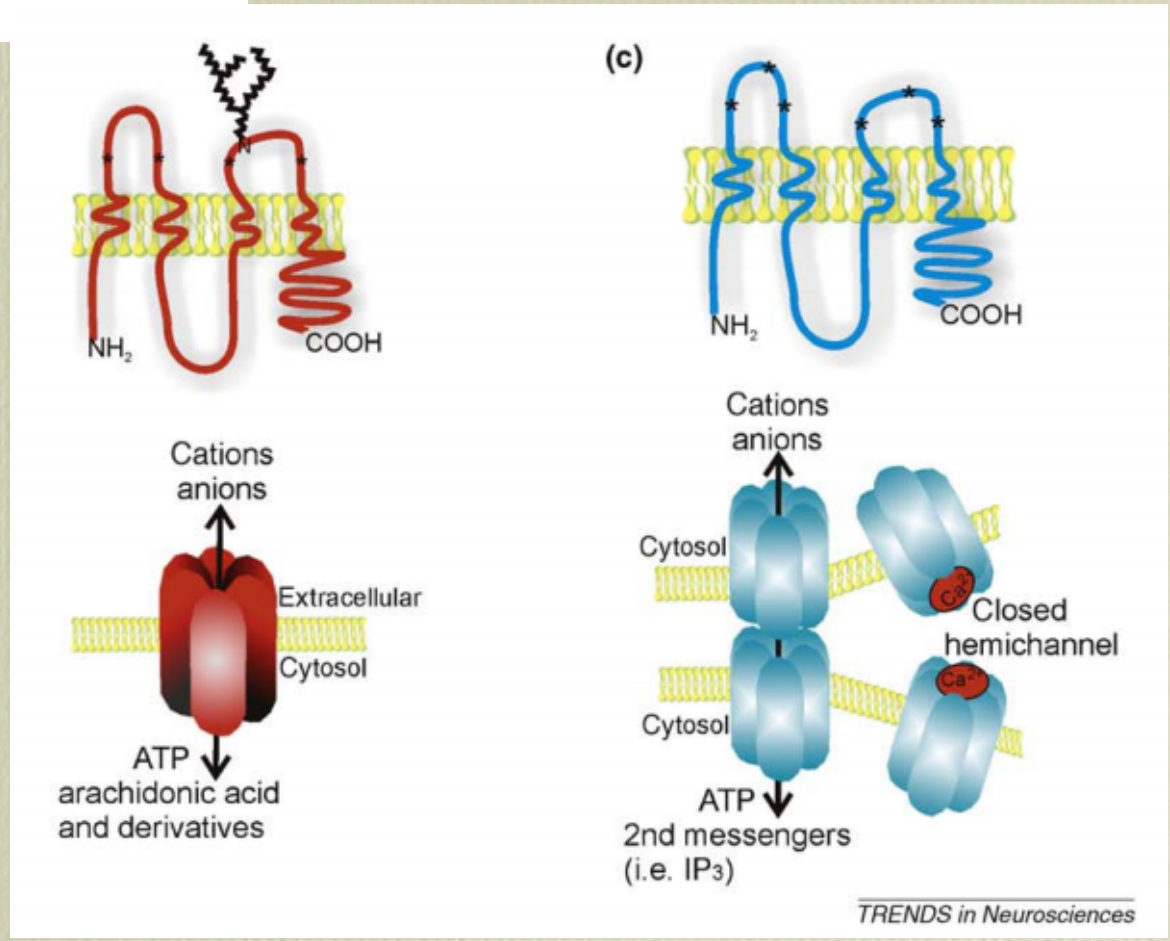
NH2
COOH
Cations
anions
Extracellular
Cytosol
ATP
arachidonic acid
and derivatives
(c)
NH2
COOH
Cations
anions
Cytosol
Closed
hemichannel
Cytosol
ATP
2nd messengers
(i.e. IP3)
TRENDS in Neurosciences

ARTICLES

nature medicine

Bitter taste receptors on airway smooth muscle bronchodilate by localized calcium signaling and reverse obstruction

Deepak A Deshpande[1], Wayne C H Wang[1], Elizabeth L McIlmoyle[1], Kathryn S Robinett[1], Rachel M Schillinger[1], Steven S An[2], James S K Sham[3] & Stephen B Liggett[1,4]

Remember functional redundance…

‘unexpected’ protein localization

Transient receptor potential family members PKD1L3 and PKD2L1 form a candidate sour taste receptor

Yoshiro Ishimaru*, Hitoshi Inada†, Momoka Kubota*, Hanyi Zhuang*, Makoto Tominaga†‡, and Hiroaki Matsunami*¶

PNAS | August 15, 2006 | vol. 103 | no. 33 | 12569–12574

Type III cells are sensitive to acids (not H+)

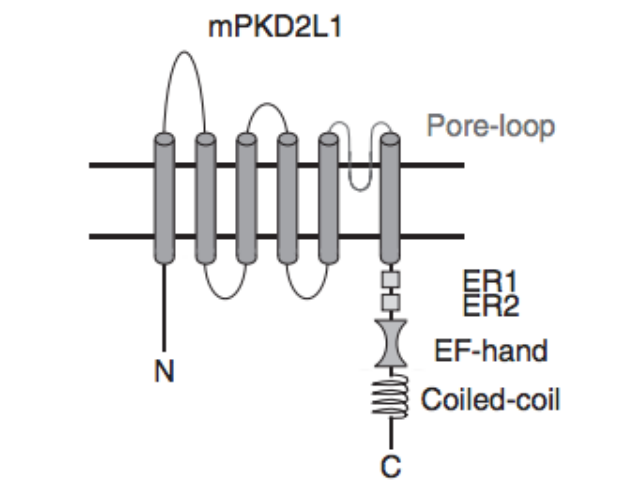

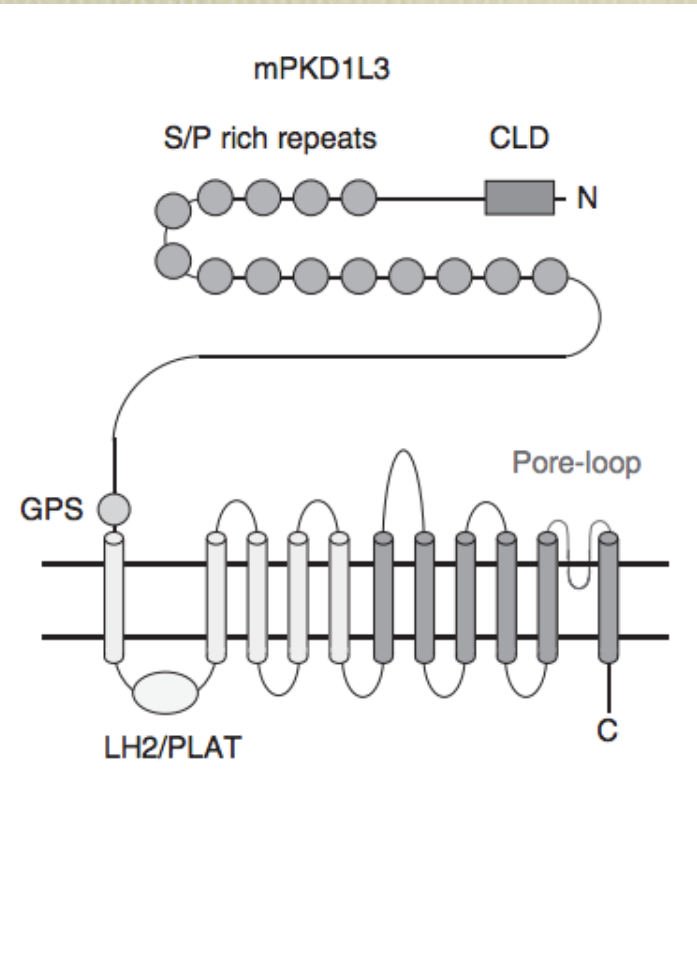

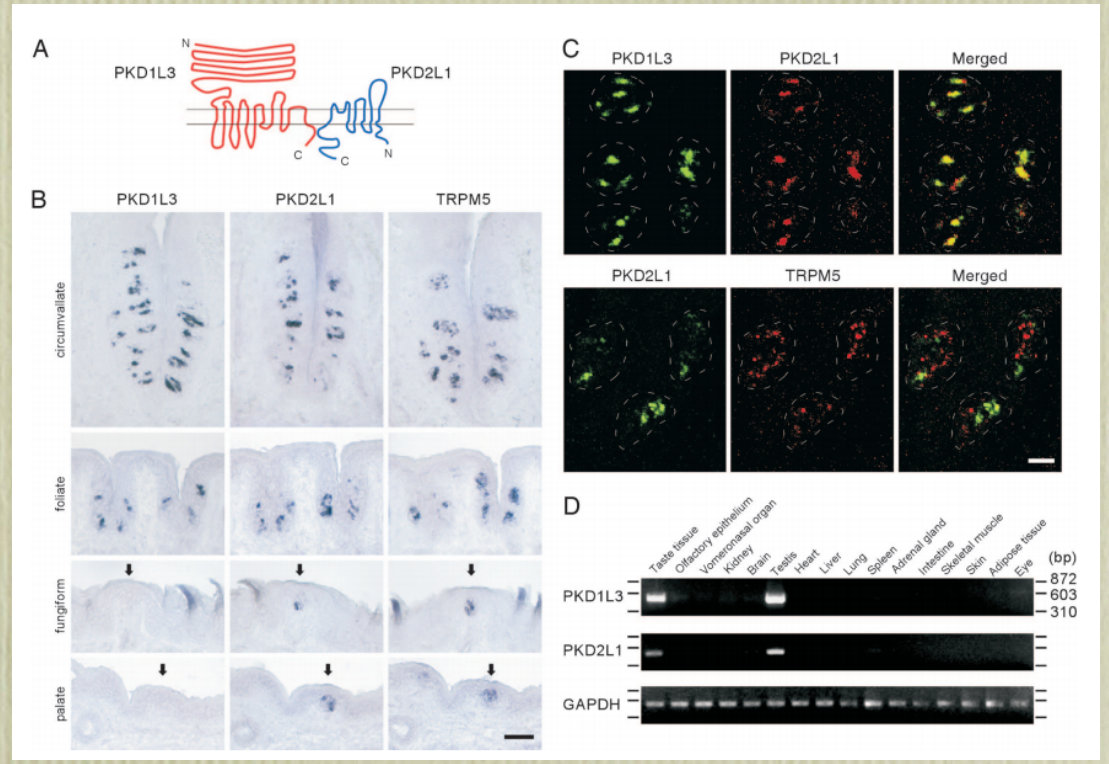
A
PKD1L3
PKD2L1
N
C
C
N
B
PKD1L3
PKD2L1
TRPM5
circumvallate
foliate
fungiform
palate
C
PKD1L3
PKD2L1
Merged
PKD2L1
TRPM5
Merged
D
Taste tissue
Olfactory epithelium
Vomeronasal organ
Kidney
Brain
Testis
Heart
Liver
Lung
Spleen
Adrenal gland
Intestine
Skeletal muscle
Skin
Adipose tissue
Eye
(bp)
872
603
310
PKD1L3
PKD2L1
GAPDH

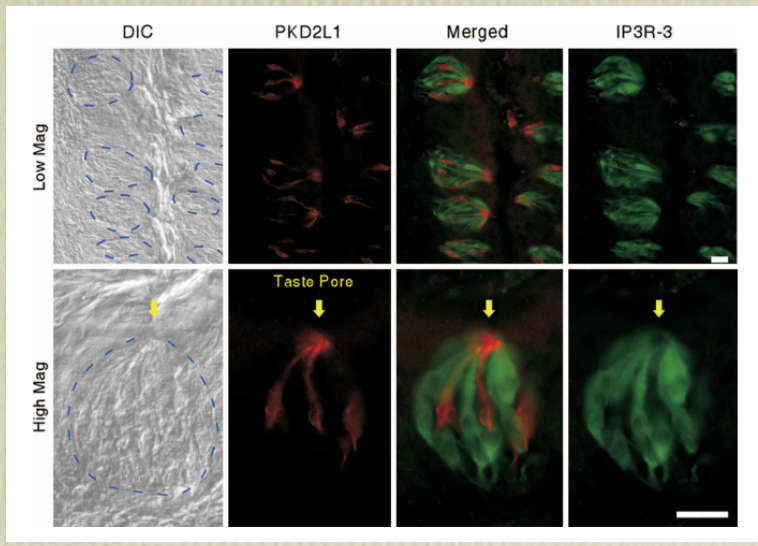
DIC
PKD2L1
Merged
IP3R-3
Low Mag
High Mag
Taste Pore

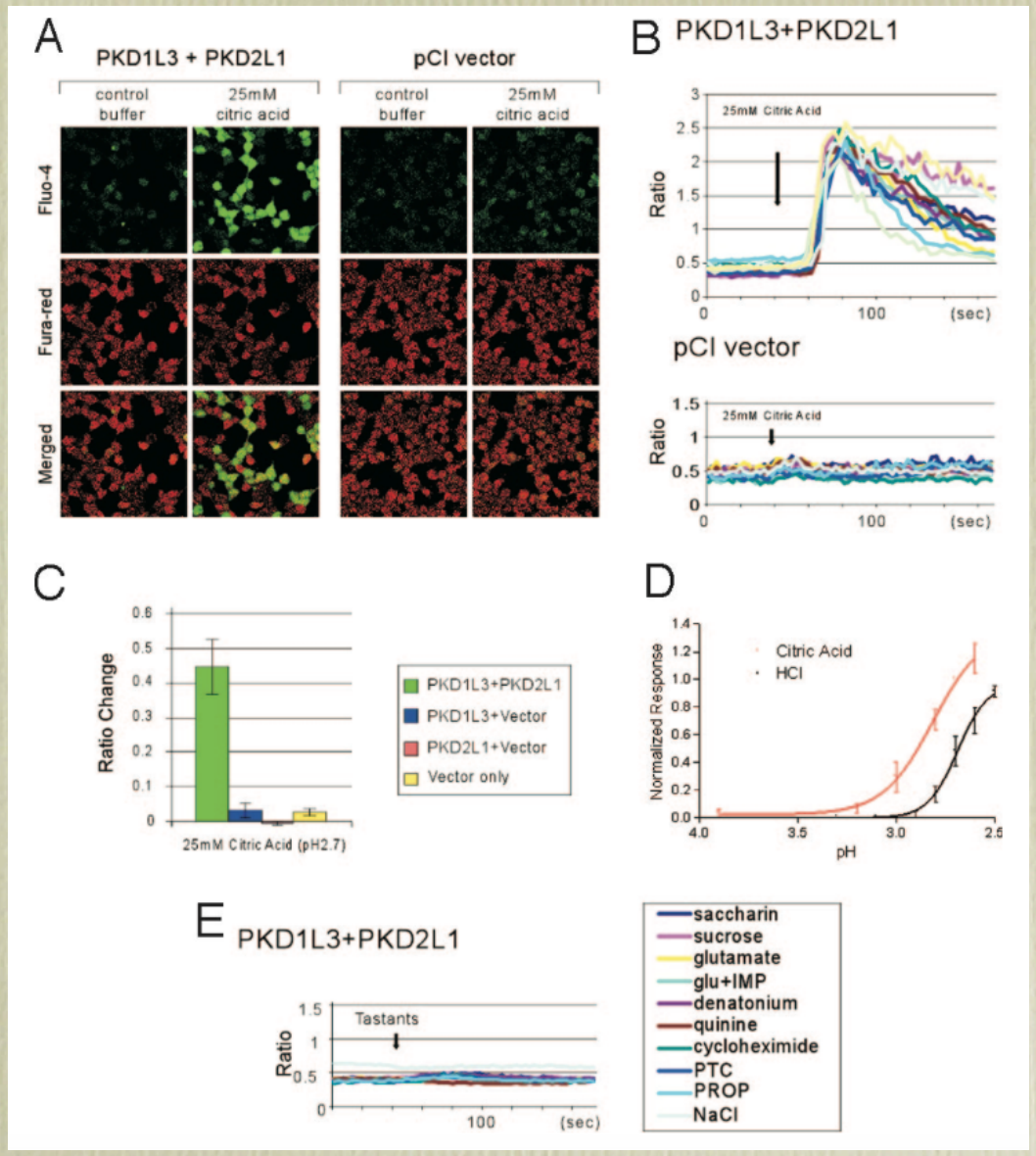
A
PKD1L3 + PKD2L1
pCI vector
control buffer
25mM citric acid
control buffer
25mM citric acid
Fluo-4
Fura-red
Merged
B
PKD1L3+PKD2L1
25mM Citric Acid
Ratio
(sec)
pCI vector
25mM Citric Acid
Ratio
(sec)
C
Ratio Change
25mM Citric Acid (pH2.7)
PKD1L3+PKD2L1
PKD1L3+Vector
PKD2L1+Vector
Vector only
D
Normalized Response
Citric Acid
HCl
pH
E
PKD1L3+PKD2L1
Tastants
Ratio
(sec)
saccharin
sucrose
glutamate
glu+IMP
denatonium
quinine
cycloheximide
PTC
PROP
NaCl

OPEN ACCESS Freely available online

PLoS one

Sour Taste Responses in Mice Lacking PKD Channels

Nao Horio[1☯], Ryusuke Yoshida[1☯], Keiko Yasumatsu[1,2], Yuchio Yanagawa[3,4], Yoshiro Ishimaru[5,6], Hiroaki Matsunami[6], Yuzo Ninomiya[1]*

Conclusions/Significance: These findings suggest that PKD2L1 partly contributes to sour taste responses in mice and that receptors other than PKDs would be involved in sour detection.

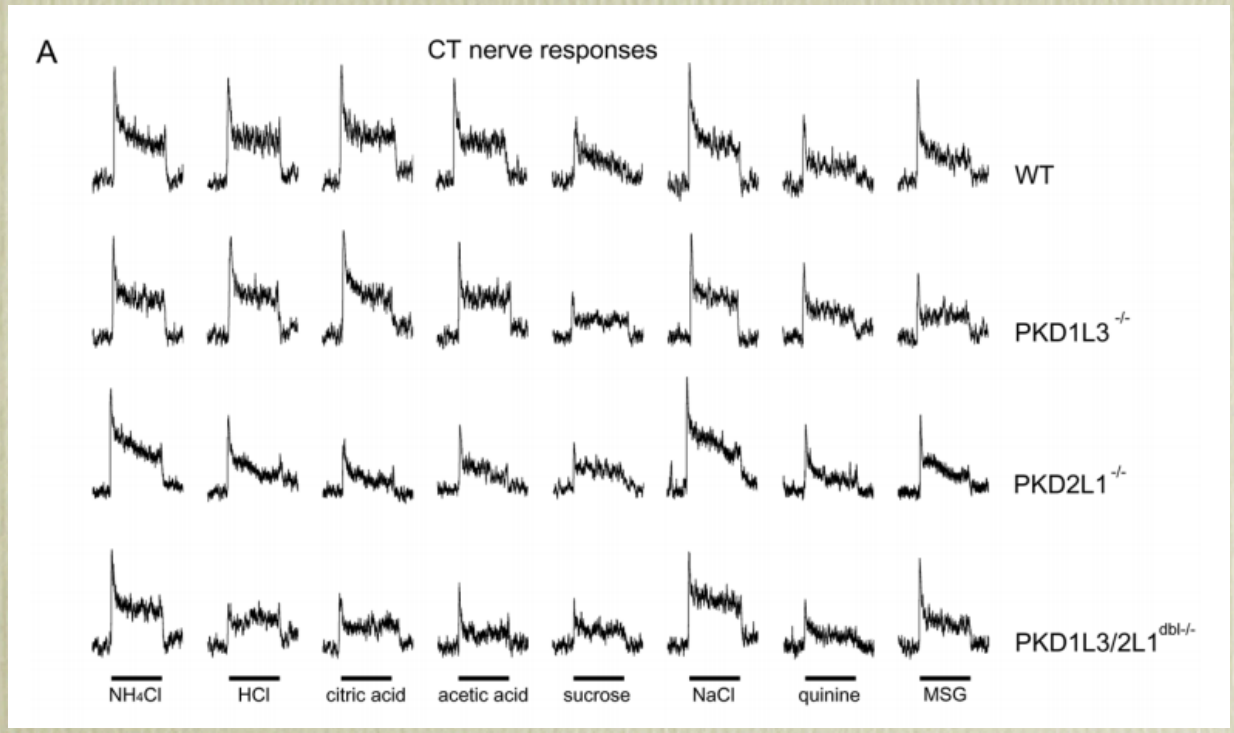

Table 3. ANOVA results for CT and GL nerve responses to taste compounds (vs. WT mice) (Horio et al.).

		PKD1L3$^{-/-}$		PKD2L1$^{-/-}$		PKD1L3/2L1$^{dbl-/-}$	
nerve	**tastant**	**DF**	**F**	**DF**	**F**	**DF**	**F**
CT	HCl	1,64	0.2	1,74	30.1***	1,69	12.1***
	CA	1,64	1.6	1,74	20.9***	1,69	14.5***
	AA	1,64	2.4	1,74	22.5***	1,69	12.0***
	Suc	1,64	2.1	1,74	0.4	1,69	1.4
	NaCl	1,64	2.0	1,74	0.0	1,69	2.8
	QHCl	1,64	1.5	1,74	1.3	1,69	3.8
	MSG	1,64	0.2	1,74	0.0	1,69	0.3
	MPG	1,64	0.0	1,74	0.7	1,69	2.9
GL	HCl	1,69	0.7	1,69	0.0	1,69	0.0
	CA	1,69	0.2	1,69	3.8	1,69	0.6
	AA	1,69	0.9	1,69	3.8	1,69	2.9
	Suc	1,69	1.7	1,69	0.6	1,69	2.3
	NaCl	1,69	0.6	1,69	2.2	1,69	0.2
	QHCl	1,69	3.8	1,69	3.4	1,69	0.4
	MSG	1,69	0.3	1,69	3.4	1,69	0.7
	MPG	1,69	2.6	1,69	0.7	1,69	2.7

Response magnitudes were analyzed by two-way ANOVA. Table based on data shown in Fig. 4. DF: degree of freedom. F: F values.
***: $P<0.001$, ANOVA.
doi:10.1371/journal.pone.0020007.t003

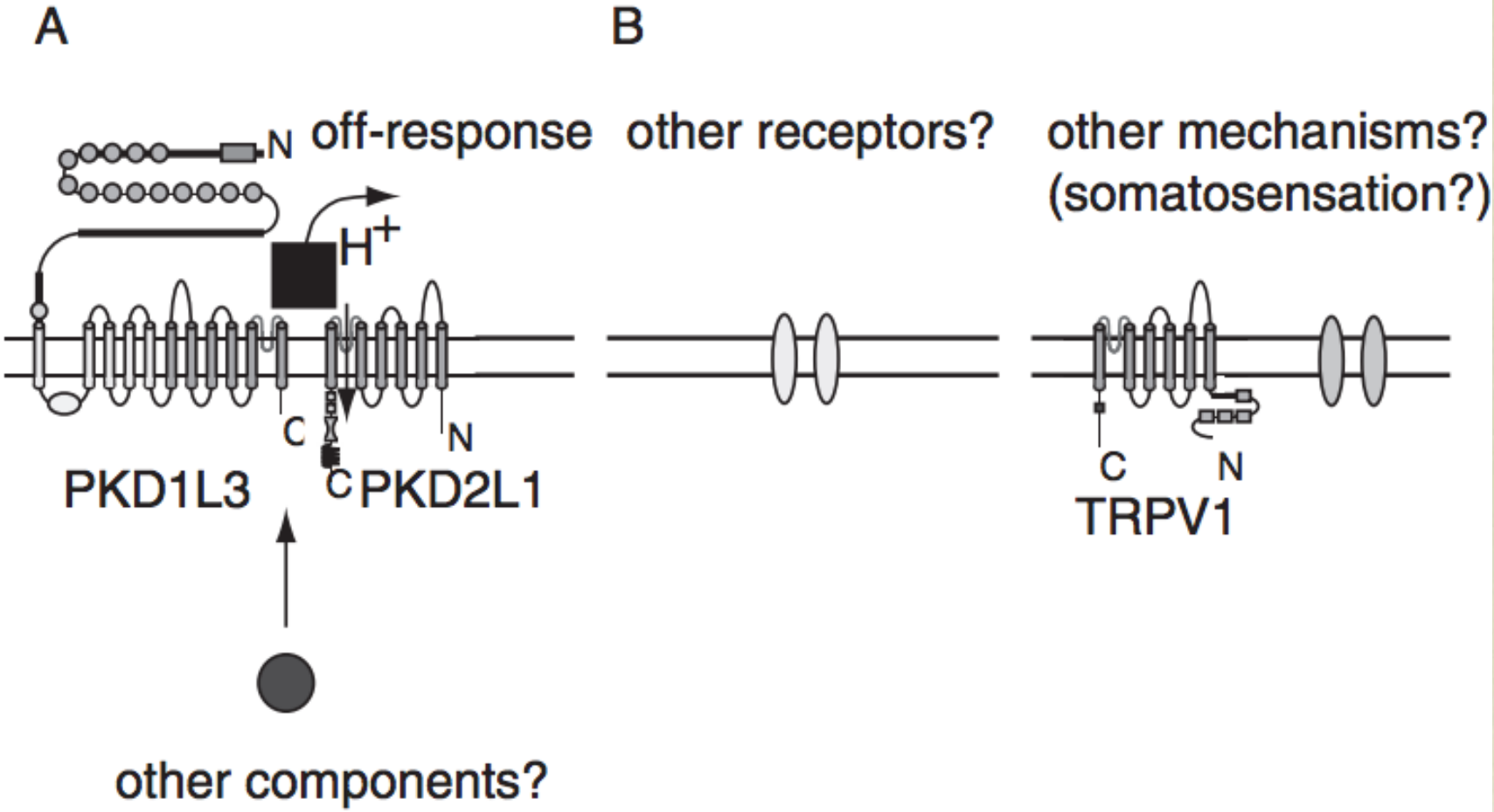
A
B
N
off-response
other receptors?
other mechanisms?
(somatosensation?)
H+
C
N
PKD1L3
C
PKD2L1
C
N
TRPV1
other components?

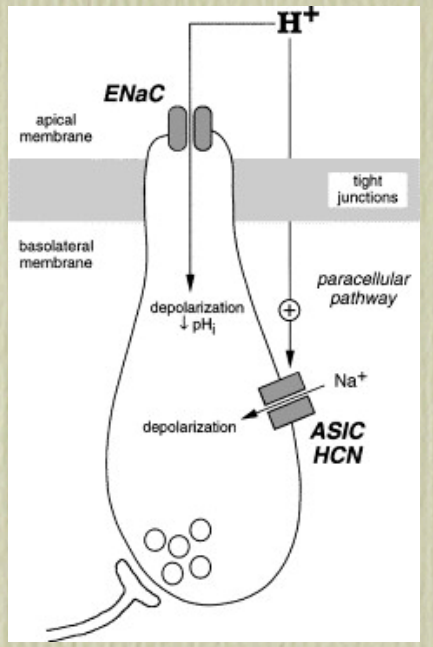
H+
ENaC
apical membrane
tight junctions
basolateral membrane
paracellular pathway
depolarization
↓ pHi
Na+
depolarization
ASIC
HCN

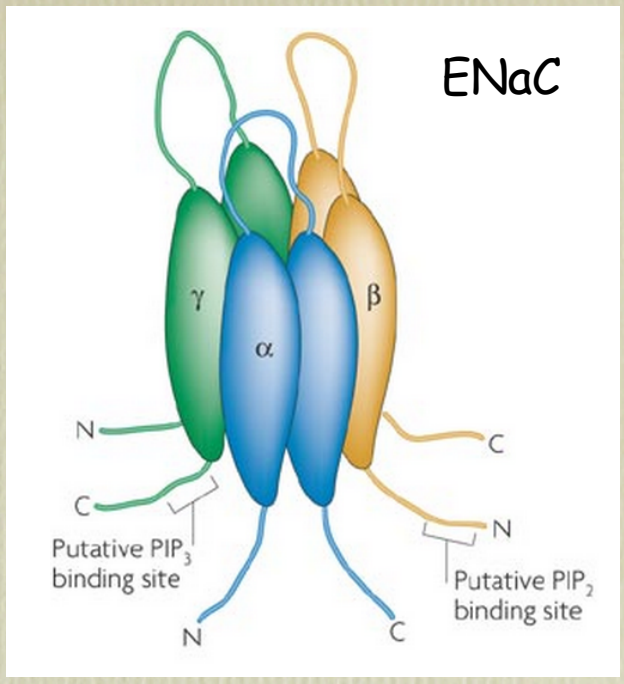
ENaC
γ
α
β
N
C
C
N
Putative PIP3 binding site
Putative PIP2 binding site
N
C

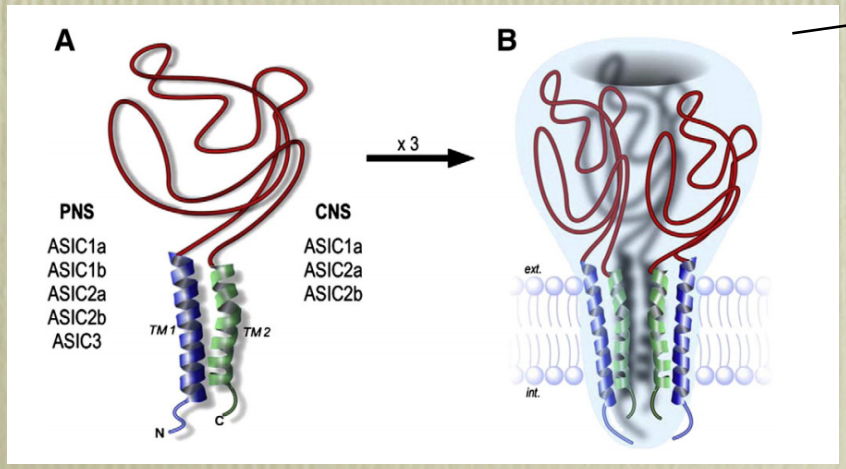
A
B
x 3
PNS
ASIC1a
ASIC1b
ASIC2a
ASIC2b
ASIC3
CNS
ASIC1a
ASIC2a
ASIC2b
TM 1
TM 2
N
C
ext.
int.

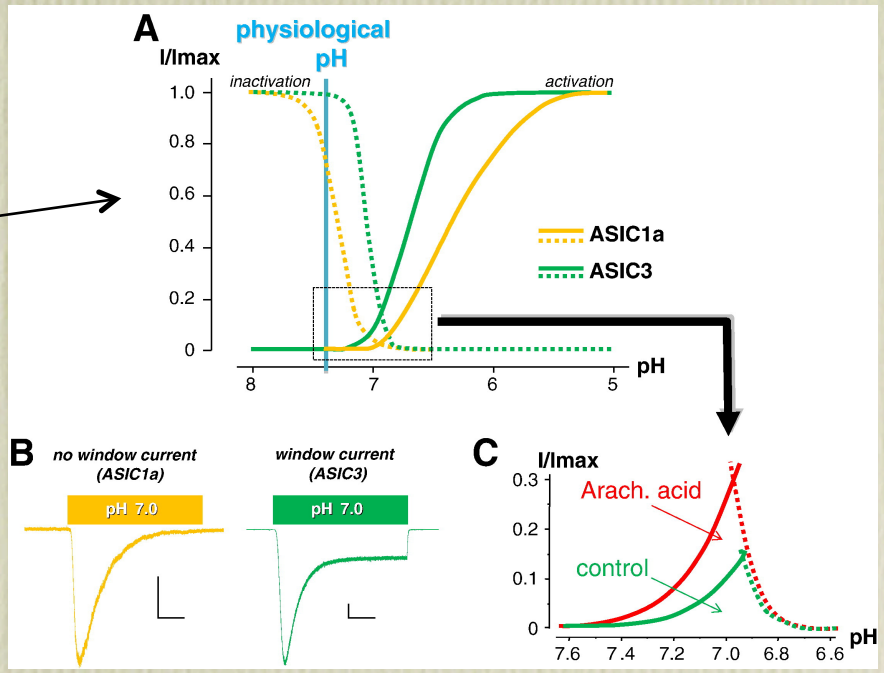
A
physiological pH
I/Imax
inactivation
activation
1.0
0.8
0.6
0.4
0.2
0
8
7
6
5
pH
ASIC1a
ASIC3
B
no window current (ASIC1a)
window current (ASIC3)
pH 7.0
pH 7.0
C
I/Imax
Arach. acid
control
0.3
0.2
0.1
0
7.6
7.4
7.2
7.0
6.8
6.6
pH

OLFACTION

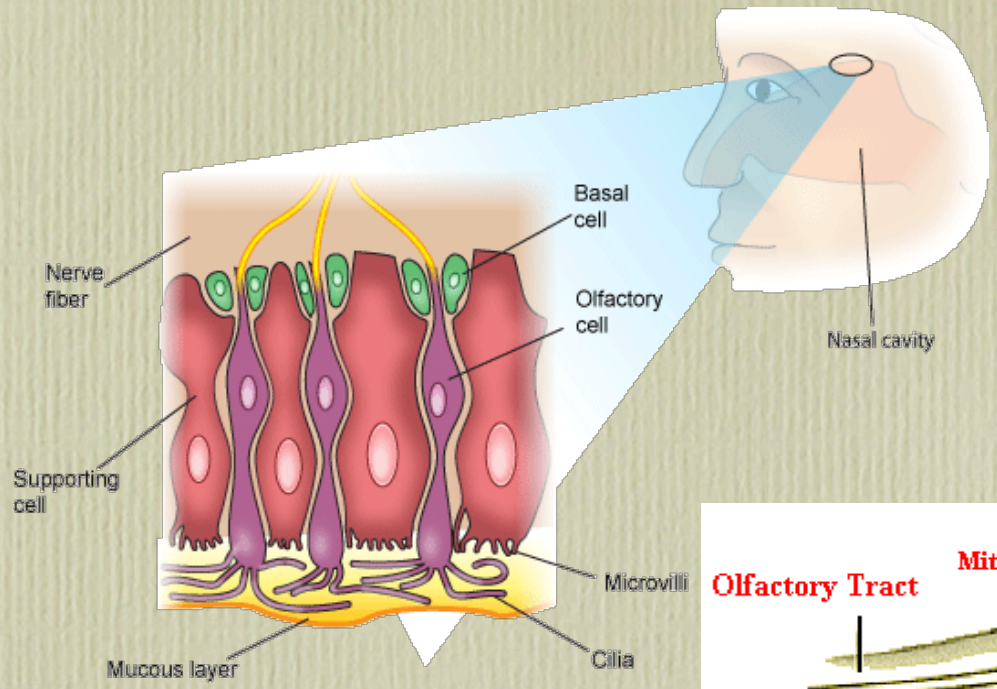
Basal cell
Nerve fiber
Olfactory cell
Nasal cavity
Supporting cell
Microvilli
Cilia
Mucous layer


RF
RC
RM
RM
RC
RC

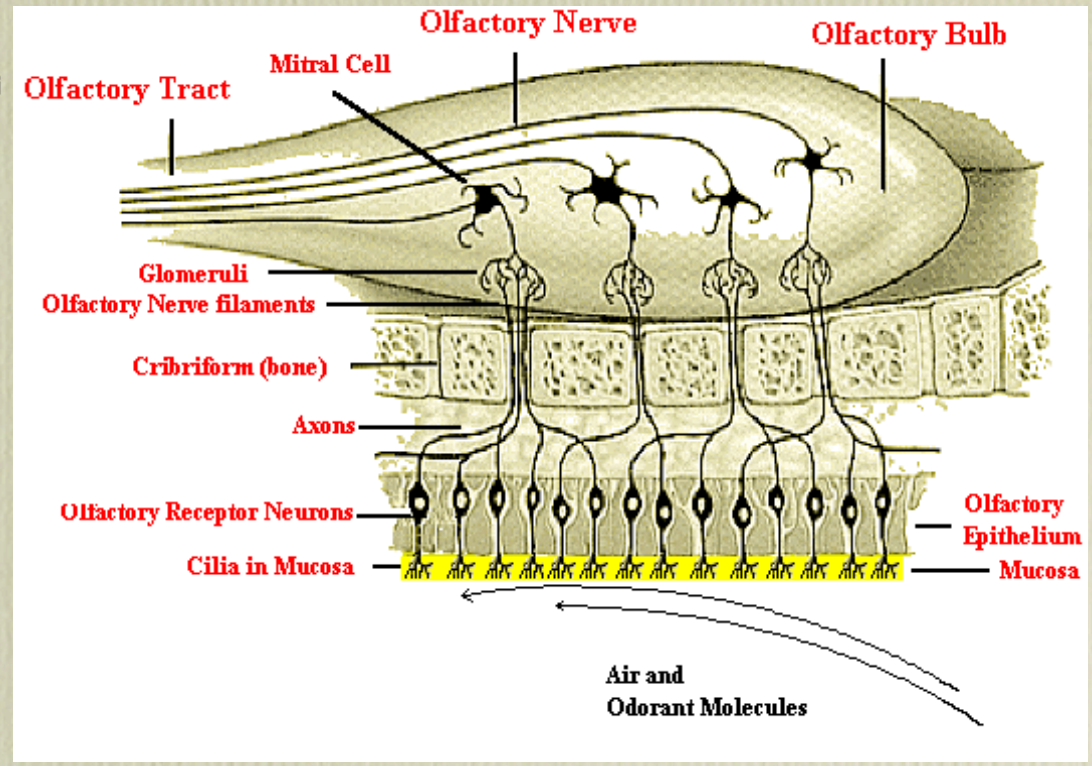
Olfactory Nerve
Olfactory Bulb
Mitral Cell
Olfactory Tract
Glomeruli
Olfactory Nerve filaments
Cribriform (bone)
Axons
Olfactory Receptor Neurons
Olfactory Epithelium
Cilia in Mucosa
Mucosa
Air and
Odorant Molecules

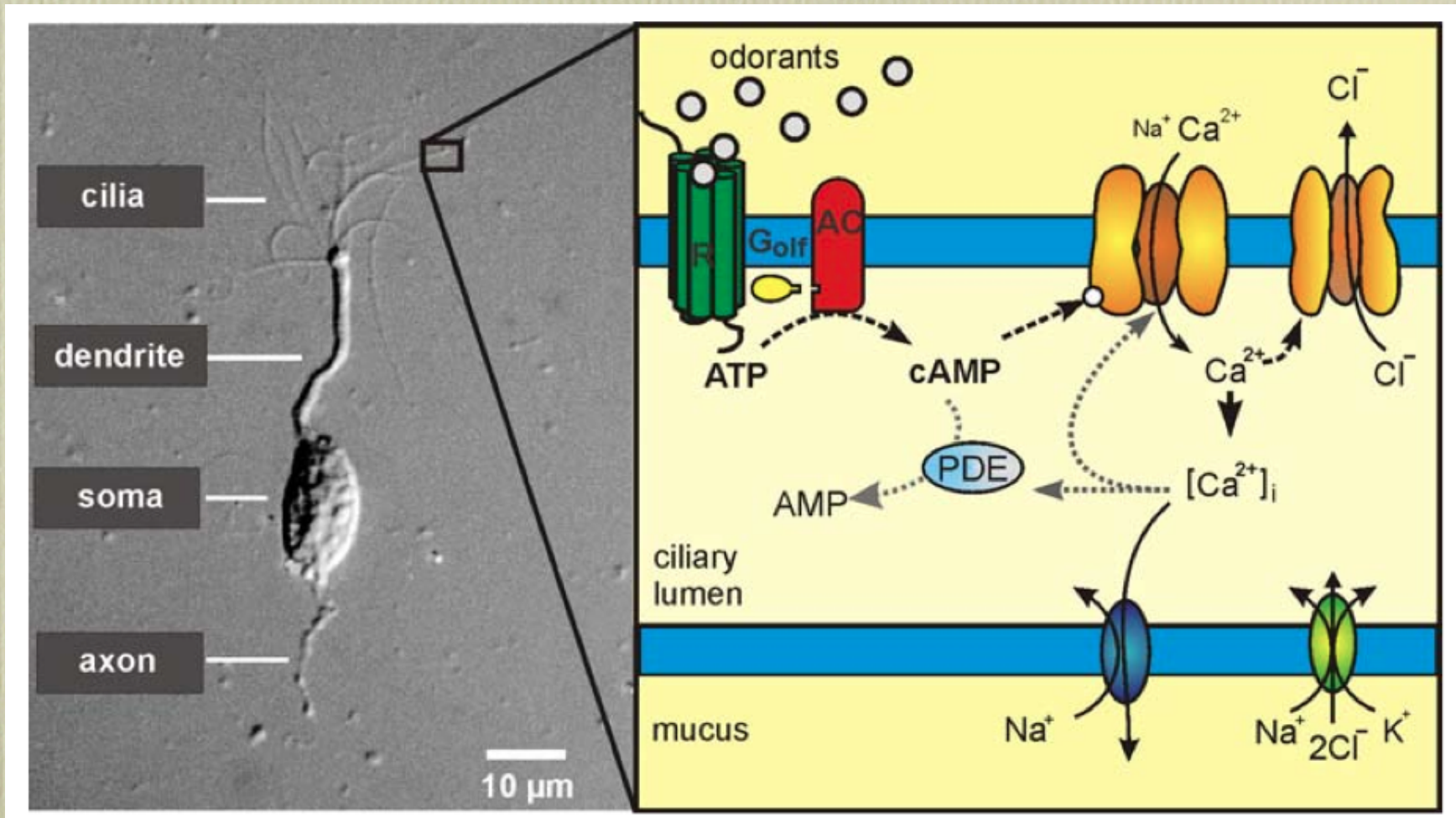
cilia
dendrite
soma
axon
10 µm
odorants
R
Golf
AC
ATP
cAMP
Na+ Ca2+
Cl−
Ca2+
Cl−
PDE
AMP
[Ca2+]i
ciliary lumen
mucus
Na+
Na+ 2Cl− K+

nature neuroscience

Ca^{2+}-activated Cl^- currents are dispensable for olfaction

Gwendolyn M Billig[1,2], Balázs Pál[1], Pawel Fidzinski[1] & Thomas J Jentsch[1,3]

Canonical olfactory signal transduction involves the activation of cyclic AMP–activated cation channels that depolarize the cilia of receptor neurons and raise intracellular calcium. Calcium then activates Cl^- currents that may be up to tenfold larger than cation currents and are believed to powerfully amplify the response. We identified Anoctamin2 (Ano2, also known as TMEM16B) as the ciliary Ca^{2+}-activated Cl^- channel of olfactory receptor neurons. Ano2 is expressed in the main olfactory epithelium (MOE) and in the vomeronasal organ (VNO), which also expresses the related Ano1 channel. Disruption of *Ano2* in mice virtually abolished Ca^{2+}-activated Cl^- currents in the MOE and VNO. *Ano2* disruption reduced fluid-phase electro-olfactogram responses by only ~40%, did not change air-phase electro-olfactograms and did not reduce performance in olfactory behavioral tasks. In contrast with the current view, cyclic nucleotide–gated cation channels do not need a boost by Cl^- channels to achieve near-physiological levels of olfaction.

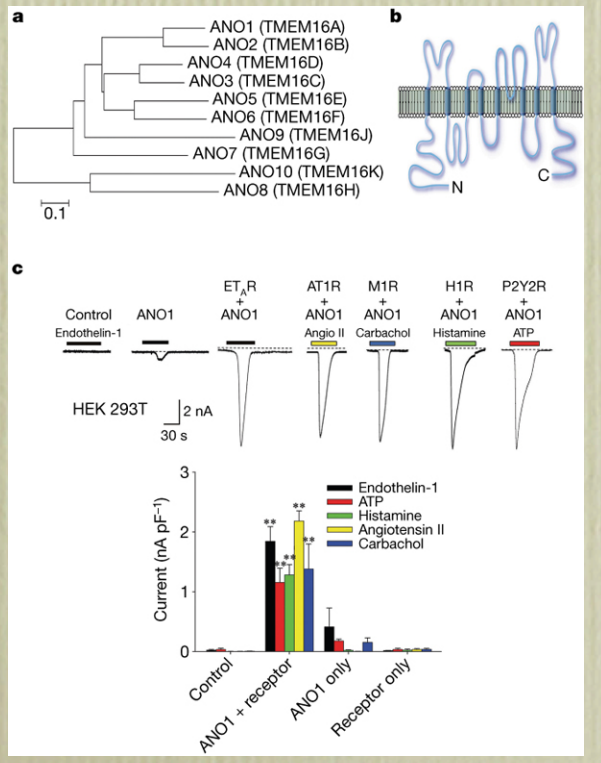

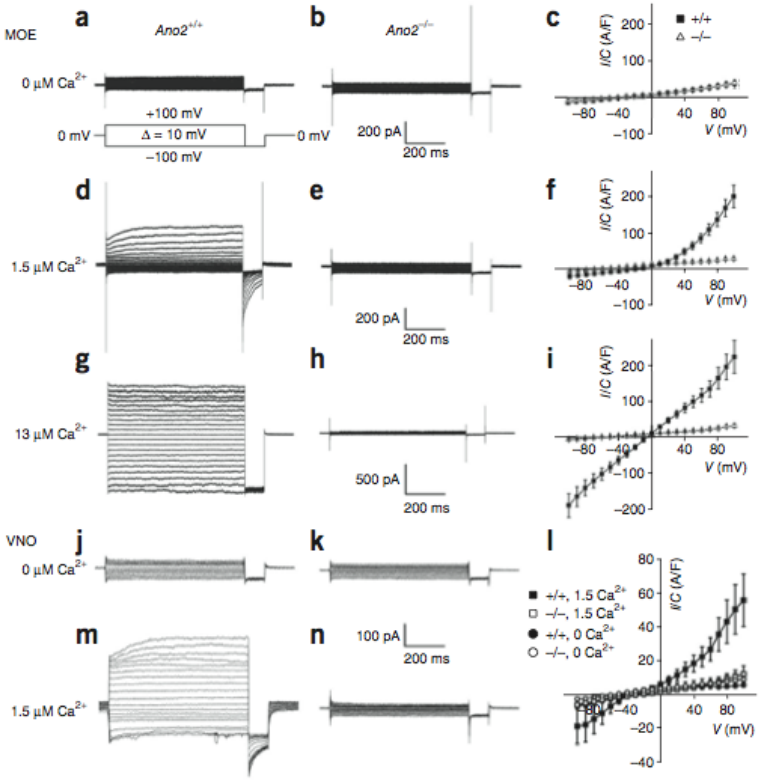

Figure 5 Effect of *Ano2* disruption on Ca^{2+}-activated Cl^- currents. Patch-clamp recordings of olfactory receptor neurons from the MOE (**a**–**i**) and the VNO (**j**–**l**). (**a**,**d**,**g**) Typical current traces obtained from *Ano2*$^{+/+}$ OSNs in the presence of nominally 0 μM, 1.5 μM and 13 μM Ca^{2+} in the recording pipette, respectively. The voltage-clamp protocol is shown in **a**. (**b**,**e**,**h**) Current densities (*I*/*C*) from *Ano2*$^{-/-}$ OSNs under conditions as in **a**,**d**,**g**. (**c**,**f**,**i**) Averaged current-voltage relationships of steady-state currents with 0 μM, 1.5 μM and 13 μM Ca^{2+} in the pipette, respectively. ■ wild-type cells, Δ *Ano2*$^{-/-}$ cells. Error bars, s.e.m. Number of cells measured: (**c**) 7 wild type, 7 knockout; (**f**), 15 wild type, 11 knockout; (**i**), 14 wild type, 10 knockout. (**j**,**m**) Typical current traces of wild-type vomeronasal sensory neurons (VSNs) with 0 μM Ca^{2+} (**j**) and 1.5 μM free Ca^{2+} (**m**) in the pipette. (**k**) *Ano2*$^{-/-}$ VSN with 0 μM Ca^{2+}, and (**n**) with 1.5 μM Ca^{2+} in the pipette. (**l**) Averaged current-voltage relationships from VNO receptor neurons measured with 1.5 μM Ca^{2+} (■ *Ano2*$^{+/+}$, □ *Ano2*$^{-/-}$; $n = 7$ and 6, respectively) and with 0 μM Ca^{2+} (● wild type, ○ *Ano2*$^{-/-}$; $n = 5$ for both). Error bars, s.e.m. Voltage clamp protocol as in **a**.

larger. Averaged current/voltage curves revealed that Ca^{2+}-activated Cl^- currents of VSNs depend predominantly on Ano2 (**Fig. 5l**). Although Ano1 is expressed in the VNO (**Fig. 3a**), its contribution to VSN currents seems minor.

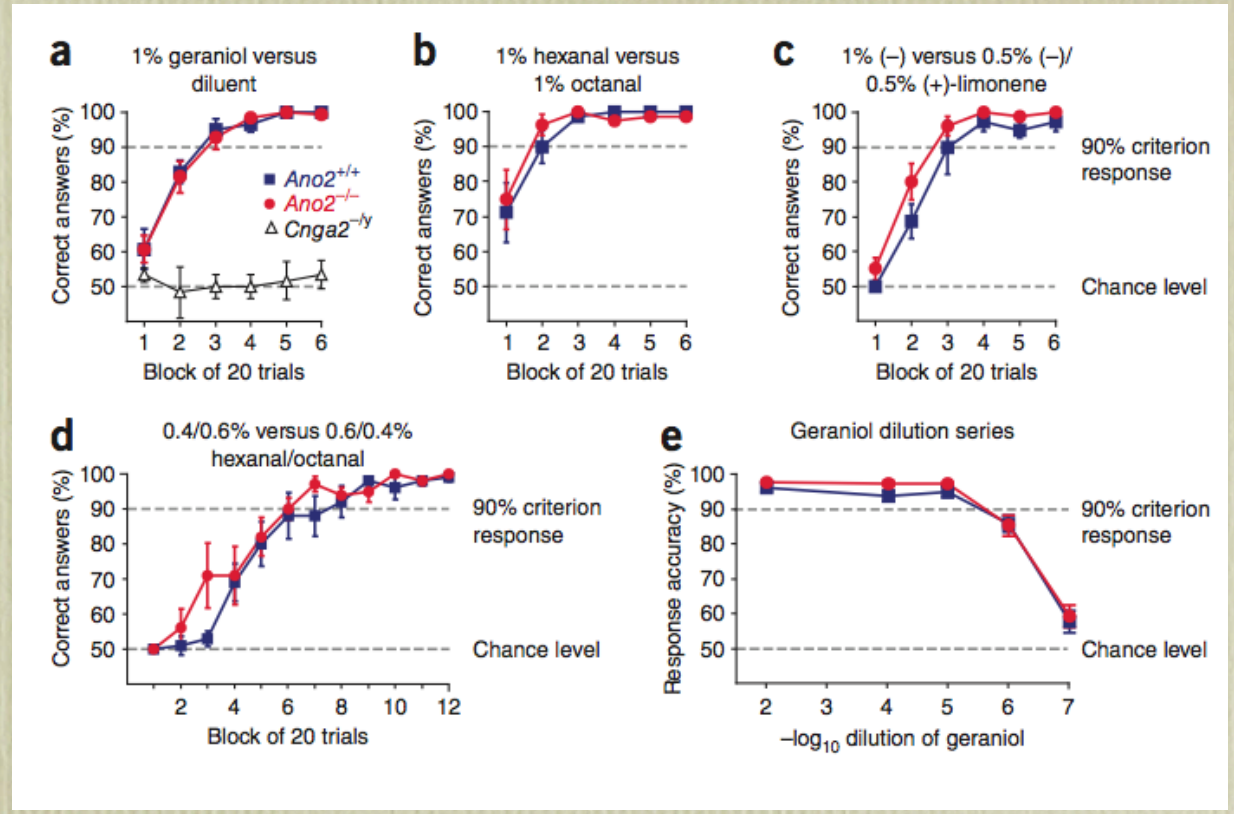

Figure 8 *Ano2* disruption affected neither odor discrimination nor olfactory sensitivity. (**a**–**d**) Different discrimination tasks. As true for wild-type littermates, $Ano2^{-/-}$ mice learned to discriminate between 1% geraniol and the diluent mineral oil ($n = 6$ for each genotype) (**a**), between 1% hexanal and 1% octanal ($n = 3$ for each genotype) (**b**), between 1% (–)-limonene and an enantiomeric mixture of 0.5% (–)-limonene and 0.5% (+)-limonene ($n = 4$ for each genotype) (**c**) and between 0.4% hexanal/0.6% octanal and 0.6% hexanal/0.4% octanal ($n = 5$ for each genotype) (**d**). Anosmic $Cnga2^{-/y}$ mice ($n = 3$) could not detect 1% geraniol (**a**). (**e**) Odor detection threshold for geraniol. Both $Ano2^{-/-}$ ($n = 6$) and $Ano2^{+/+}$ littermates ($n = 6$) detected geraniol and discriminated it from the diluent only down to a dilution of 10^{-6}. The first data point with a geraniol dilution of 10^{-2} corresponds to **a**. Error bars, s.e.m. There was no significant difference between $Ano2^{+/+}$ and $Ano2^{-/-}$ mice in any of these tests.

On the scent of mitochondrial calcium

Frank Zufall

Odorants are now shown to elevate mitochondrial Ca^{2+} in sensory neurons; moreover, blocking this Ca^{2+} sequestration impairs dynamic range. Acute stimulation rapidly recruits mitochondria from the soma to the dendritic knob.

ARTICLES

nature neuroscience

Mitochondrial Ca^{2+} mobilization is a key element in olfactory signaling

Daniela Fluegge[1,5], Lisa M Moeller[1,5], Annika Cichy[1], Monika Gorin[1], Agnes Weth[2], Sophie Veitinger[1], Silvia Cainarca[3], Stefan Lohmer[3], Sabrina Corazza[3], Eva M Neuhaus[4], Werner Baumgartner[2], Jennifer Spehr[1] & Marc Spehr[1]

In olfactory sensory neurons (OSNs), cytosolic Ca^{2+} controls the gain and sensitivity of olfactory signaling. Important components of the molecular machinery that orchestrates OSN Ca^{2+} dynamics have been described, but key details are still missing. Here, we demonstrate a critical physiological role of mitochondrial Ca^{2+} mobilization in mouse OSNs. Combining a new mitochondrial Ca^{2+} imaging approach with patch-clamp recordings, organelle mobility assays and ultrastructural analyses, our study identifies mitochondria as key determinants of olfactory signaling. We show that mitochondrial Ca^{2+} mobilization during sensory stimulation shapes the cytosolic Ca^{2+} response profile in OSNs, ensures a broad dynamic response range and maintains sensitivity of the spike generation machinery. When mitochondrial function is impaired, olfactory neurons function as simple stimulus detectors rather than as intensity encoders. Moreover, we describe activity-dependent recruitment of mitochondria to olfactory knobs, a mechanism that provides a context-dependent tool for OSNs to maintain cellular homeostasis and signaling integrity.

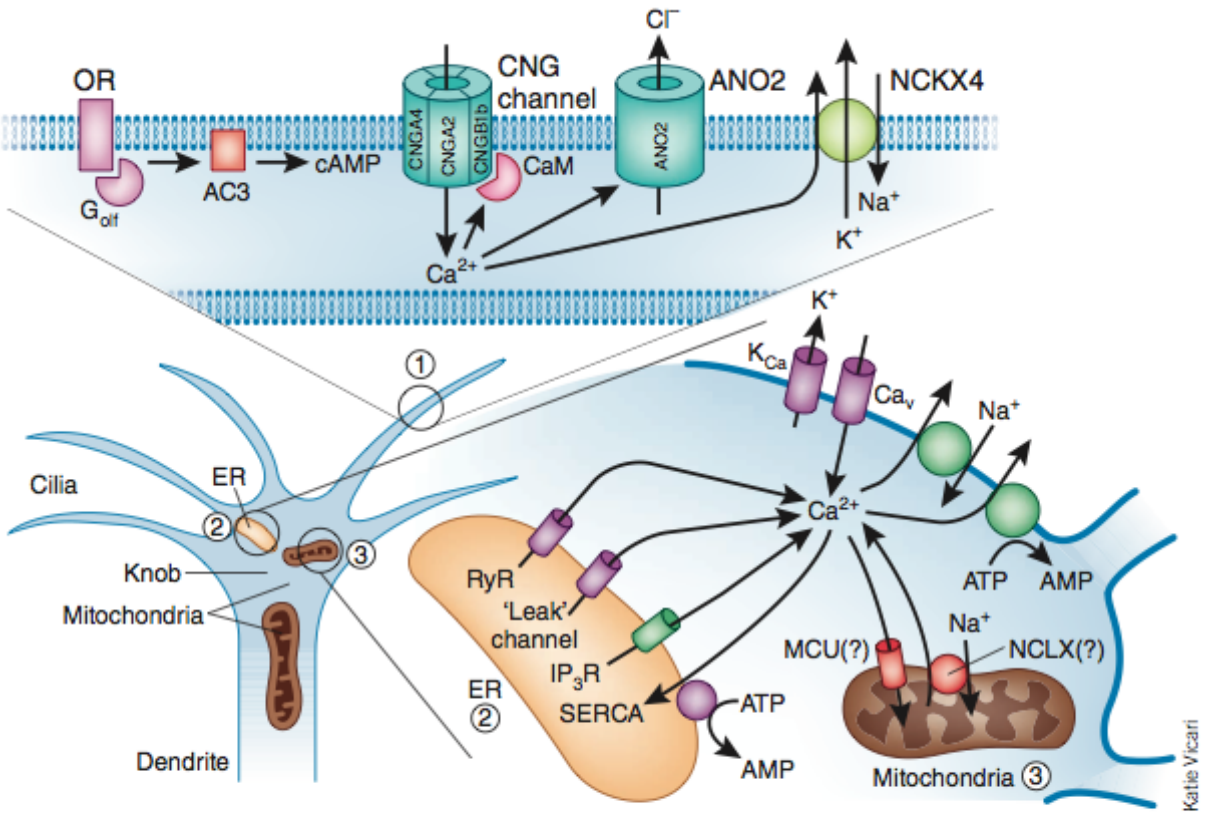

Figure 1 Schematic representation of Ca^{2+} signaling mechanisms in cilia and dendritic knob of an OSN. Much is known about the main Ca^{2+} influx pathway in the cilia (1), the role of Ca^{2+} in primary olfactory signal transduction, and the principal Na^+/Ca^{2+} exchanger (NCKX4) that allows rapid response termination and adaptation of an OSN[2–5,8,11]. Odor-evoked Ca^{2+} signaling in the dendritic knob and dendrite (2) involves additional Ca^{2+} regulation mechanisms, including caffeine-sensitive endoplasmic reticulum (ER) Ca^{2+} stores, Ca^{2+}-induced Ca^{2+} release and voltage-activated (Ca_V) Ca^{2+} channels[13]. However, an entire piece of the puzzle, an essential role of mitochondria (3) in OSN Ca^{2+} regulation, has been missing until now. NCLX, the mitochondrial Na^+/Ca^{2+} antiporter, and MCU, the pore-forming subunit of the mitochondrial Ca^{2+} uptake channel, may participate in mitochondrial Ca^{2+} flux[14], with the caveat that molecular proof of their presence in OSNs is still lacking. AC3, adenylyl cyclase 3; ANO2, Ca^{2+}-activated Cl^- channel; CaM, calmodulin; CNG, cyclic nucleotide gated; G_{olf}, G protein; IP_3R, inositol-1,4,5-trisphosphate receptor; K_{Ca}, Ca^{2+}-activated K^+ channel; OR, odor receptor; RyR, ryanodine receptor; SERCA, sarcoplasmic-endoplasmic reticulum Ca^{2+}-ATPase.

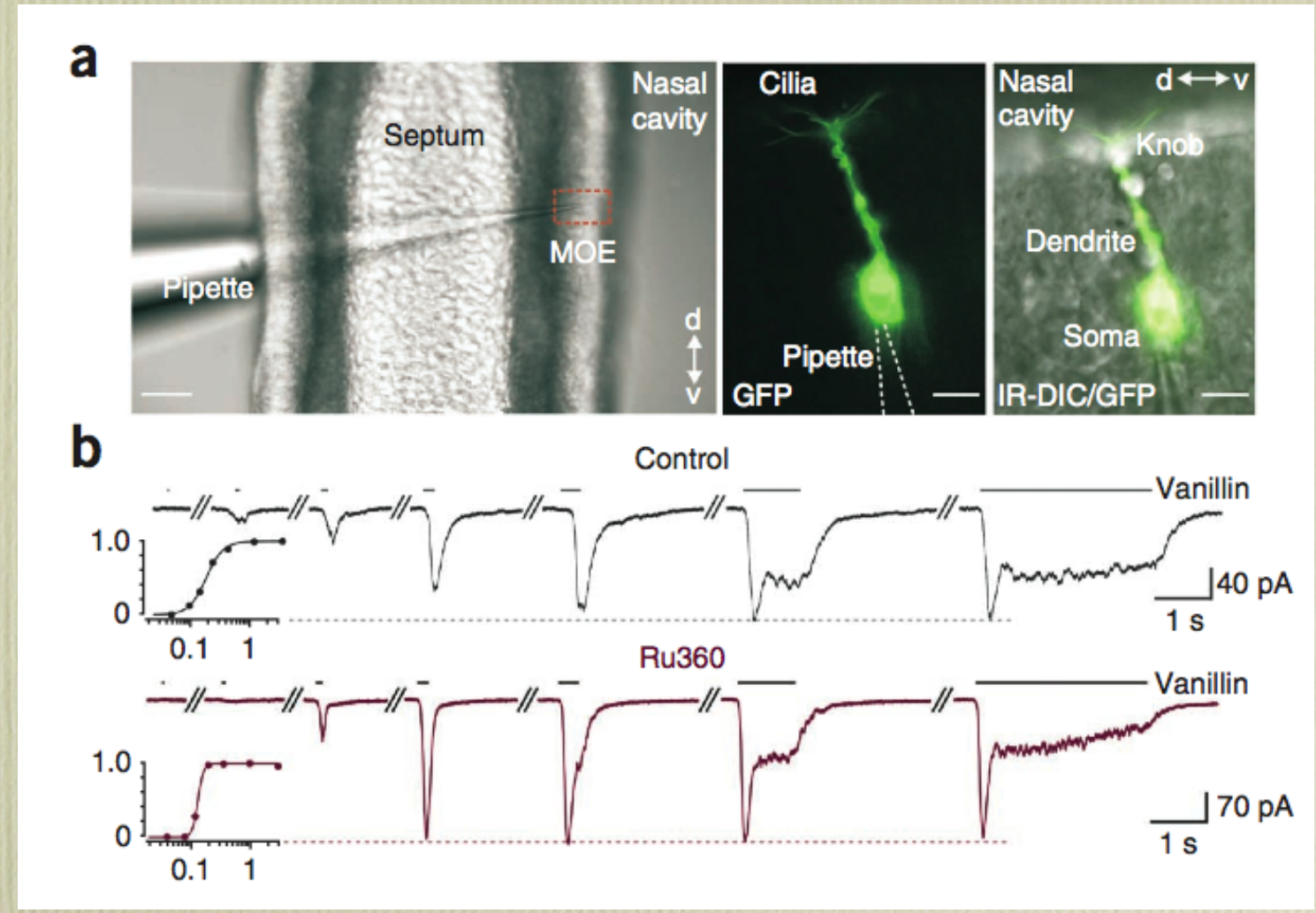
a
Septum
Nasal cavity
MOE
Pipette
d
v
Cilia
Pipette
GFP
Nasal cavity
d ⟷ v
Knob
Dendrite
Soma
IR-DIC/GFP
b
Control
Vanillin
1.0
0
0.1
1
40 pA
1 s
Ru360
Vanillin
1.0
0
0.1
1
70 pA
1 s

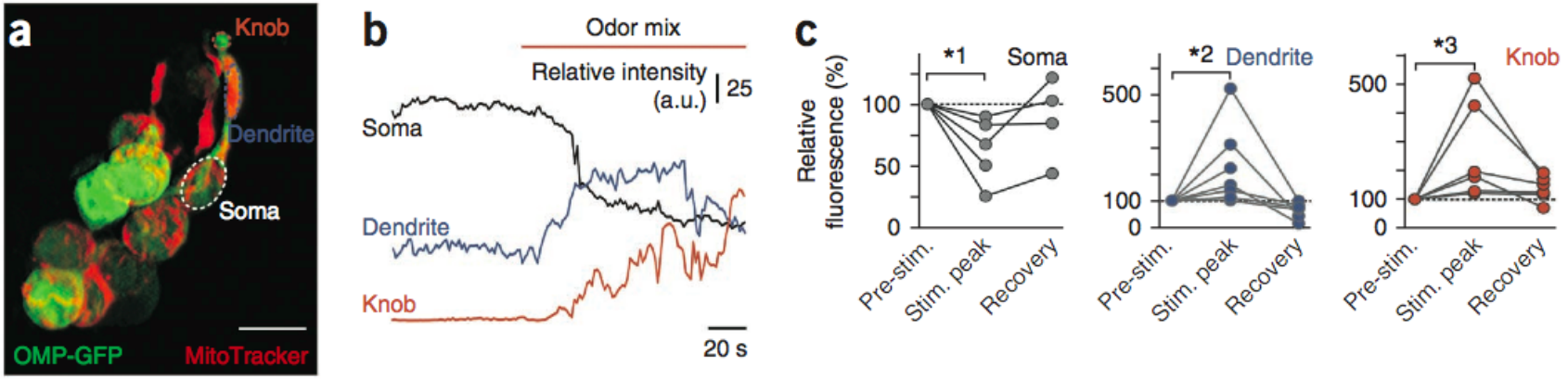
a
Knob
Dendrite
Soma
OMP-GFP
MitoTracker
b
Odor mix
Relative intensity (a.u.)
25
Soma
Dendrite
Knob
20 s
c
Relative fluorescence (%)
*1
Soma
100
50
0
Pre-stim.
Stim. peak
Recovery
*2
Dendrite
500
100
0
*3
Knob

FRAP →

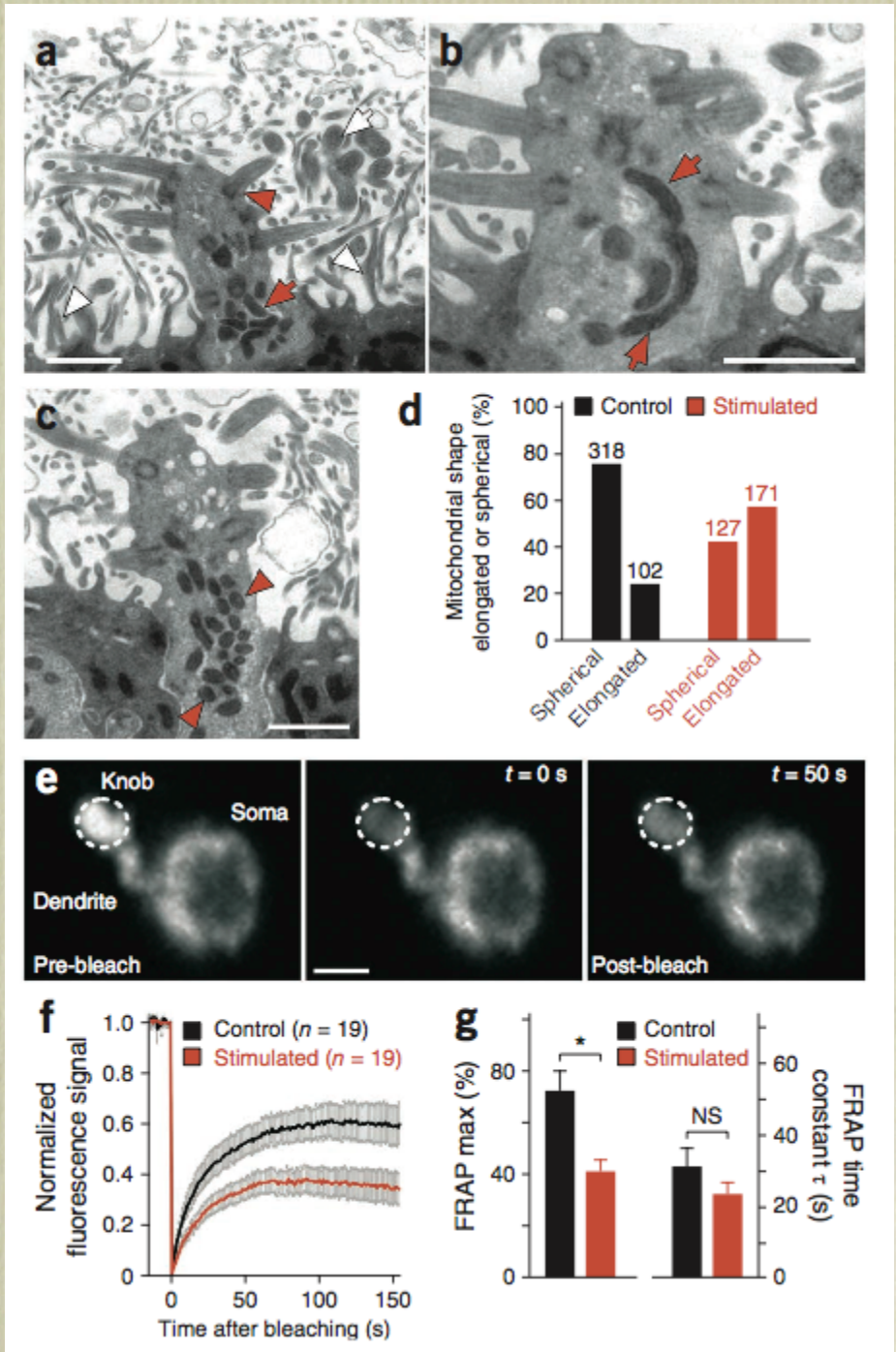
a
b
c
d
Mitochondrial shape elongated or spherical (%)
Control
Stimulated
318
102
127
171
Spherical
Elongated
Spherical
Elongated
e
Knob
Soma
Dendrite
Pre-bleach
t = 0 s
t = 50 s
Post-bleach
f
Normalized fluorescence signal
Control (n = 19)
Stimulated (n = 19)
Time after bleaching (s)
g
FRAP max (%)
Control
Stimulated
*
NS
FRAP time constant τ (s)